Report
R-15-09
November 2016

Models of C-14 in the atmosphere over vegetated land and above a surface-water body

Rodolfo Avila
Ivan Kovalets

SVENSK KÄRNBRÄNSLEHANTERING AB

SWEDISH NUCLEAR FUEL
AND WASTE MANAGEMENT CO

Box 250, SE-101 24 Stockholm
Phone +46 8 459 84 00
skb.se

SVENSK KÄRNBRÄNSLEHANTERING

ISSN 1402-3091
SKB R-15-09
ID 1555724
November 2016

Models of C-14 in the atmosphere over vegetated land and above a surface-water body

Rodolfo Avila, Ivan Kovalets
Facilia AB

Abstract

The work presented in this report is part of the biosphere modeling studies that were carried out within the SR-PSU project, dedicated to the safety assessment of the Forsmark repository for LILW. The report presents a new assessment model of the C-14 transport in the surface atmosphere above vegetated land that receives releases of this radionuclide from the soil. The model is applicable for all vegetation types that are incorporated in the SR-PSU biosphere model: crops like cereals, tubers, vegetables as well as for fodder and mire vegetation. It can be used for making predictions for relevant endpoints in a safety assessment of radioactive waste disposal facilities, such as C-14 concentrations and specific activities in the air and plants, which are used in the calculation of inhalation by humans and food ingestion doses, respectively.

The new assessment model represents an improvement with respect to the model that was used in previous safety assessments of Swedish radioactive waste disposal facilities (SAR-08 and SR-Site). The main improvement has entailed integrating explicit modelling of the turbulence driven transport of C-14 in the within and above canopy atmosphere. To keep the assessment model simple, several approximations and assumptions had to be made. A study was carried out to verify that despite the simplifications the model predictions for the endpoints of interest are sufficiently accurate, for using the model in assessments of the long-term safety of disposal facilities. The study consisted of developing a Lagrangian model, which can simulate in detail the turbulent transport of CO_2 and C-14 in the surface atmosphere in the presence of plant canopies. This model was validated using two sets of experimental data: i) CO_2 profiles in the atmosphere inside and above the canopy of a boreal forest measured in the Norunda research station in Sweden and ii) CO_2 profiles in the atmosphere above the canopy of a wheat field measured in the Agro-Ecosystems Experimental Station (AEES) located near Beijing, China. The validated Lagrangian model was then used to evaluate the assessment model by performing sensitivity studies to assess the potential impact on model predictions of simplifying assumptions inherent to the assessment model. From the evaluations made we conclude that, provided that the diffusivity coefficient at canopy top is assigned properly, the simplifying assumptions implicit in the C14-SVAT model do not lead to underestimations of the C-14 concentrations within the canopy layer, and some of them lead to moderate overestimations. From the evaluation we also identify possible ways of improving the model predictions while still keeping the model simple.

Biosphere models used in earlier safety assessments of Swedish radioactive waste disposal facilities, have not considered explicitly the processes of exchange of C-14 between surface waters and the atmosphere. These processes are not expected to be important in the context of safety assessments of disposal facilities. But nevertheless, it was decided in the SR-PSU project to model these processes explicitly and for this purpose a simple assessment model was developed, which is described in this report. The model can be used for calculation of C-14 concentrations in air above the water surface, which can be then used in estimation of inhalation doses during swimming and boating.

Contents

1 Introduction

The work presented in this report is part of the biosphere modeling studies that were carried out within the SR-PSU project, dedicated to the safety assessment of the Forsmark repository for LILW. In preceding safety assessments of Swedish radioactive waste disposal facilities (SAR-08 and SR-Site), doses from releases of C-14 to terrestrial and aquatic environments have been calculated using the models described in Avila and Pröhl (2008). One of the models in Avila and Pröhl (2008) was used for calculation of C-14 concentrations in plants resulting from C-14 releases in gas form ($^{14}CO_2$) from the ground to the canopy atmosphere and from irrigation with contaminated water. The model by Avila and Pröhl (2008), together with four other models, participated in a model comparison exercise that was carried out within the BIOPROTA project (BIOPROTA 2011). The exercise showed large discrepancies in predictions made with the compared models for the studied scenarios. The discrepancies could be explained by differences in approaches for modeling the C-14 transport in the canopy atmosphere. It was concluded from this study, that there is a need for a more rigorous modeling of these processes.

In the model described in Avila and Pröhl (2008), the vertical turbulent transport in the surface atmosphere is conservatively neglected. However, for some of the model parameters it is difficult to assign values that ensure obtaining sufficiently accurate estimates for the endpoints of interest, such as C-14 specific activities in plants. The reason for this is that the values of such parameters are influenced by a large number of factors interacting in a complex way. An example is the height of mixing in the atmosphere. In order to overcome this difficulty, an improved assessment model of the C-14 transport in the canopy atmosphere has been developed, which is described in this report. The main improvement in the model consisted of modeling explicitly the vertical transport of C-14 in the surface atmosphere driven by turbulence. This model which is called the Soil-to-Vegetation-to-Atmosphere Transport model for C-14 or the C14-SVAT model, is presented in Section 2.1. The C14-SVAT model has been incorporated into the more general biosphere model that was used in the SR-PSU safety assessment.

To keep the C14-SVAT model simple, several approximations and assumptions had to be made. A study was carried out to verify that despite the simplifications the model predictions for the end-points of interest are sufficiently accurate, for using the model in assessments of the long-term safety of disposal facilities. The study consisted of developing a Lagrangian model, described in Chapter 3, which can simulate in detail the turbulent transport of CO_2 and C-14 in the surface atmosphere in the presence of plant canopies. This model was validated using two sets of experimental data: i) CO_2 profiles in the atmosphere inside and above the canopy of a boreal forest measured in the Norunda research station (Lundin et al. 1999, Lagergren et al. 2005) in Sweden and ii) CO_2 profiles in the atmosphere above the canopy of a wheat field measured in the Agro-Ecosystems Experimental Station (AEES) located near Beijing, China. The results of the validation studies are presented in Chapter 4. Finally, the validated Lagrangian model was used to evaluate the C14-SVAT model by comparing predictions made with the two models and by performing sensitivity studies to assess the potential impact on model predictions of simplifying assumptions inherent to the C14-SVAT model (Chapter 5).

Biosphere models used in earlier safety assessments of Swedish radioactive waste disposal facilities, have not considered explicitly the processes of exchange of C-14 between surface waters and the atmosphere. These processes are not expected to be important in the context of safety assessments of disposal facilities. But nevertheless, it was decided in the SR-PSU project to model these processes explicitly and for this purpose a simple model was developed, which is described in Section 2.2. This model is called the Water-to-Atmosphere Transport model for C-14 or the C14-WAT model.

2 Assessment models for the surface atmosphere

This chapter provides a description of the assessment models that were developed within the SR-PSU project for calculating activity concentrations and specific activities of C-14 in the near-surface atmosphere and vegetation, resulting from releases to the atmosphere from the ground or a water body. The calculated activity concentrations in air are used in the safety assessment of disposal facilities for calculation of inhalation C-14 doses, whereas the specific activities in vegetation are used in calculations of C-14 doses by food ingestion.

Two assessment models are presented below: i) for modelling the transport in the surface atmosphere of C-14 released to air from vegetated land by soil and plant leaf degassing (Section 2.1), here called the C-14 Soil-to-Vegetation-to-Atmosphere Transport model or the C14-SVAT model and ii) for C-14 releases to the atmosphere above a water body, such as a lake, driven by water degassing, here called the C-14 Water-to-Atmosphere Transport model or the C14-WAT model (Section 2.2).

2.1 The C14-SVAT model

The target endpoints of the simulations with the C14-SVAT model are C-14 specific activities (Bq/kgC) in primary producers, which are used in calculations of food ingestion doses and C-14 activity concentrations in atmospheric air (Bq/m^3), which are used in calculation of inhalation doses. The model can be used in assessments for all types of vegetation included in the biosphere model for the SR-PSU safety assessment (crops like cereals, tubers, vegetables as well as for fodder and mire vegetation), for all of which the canopy height is 1 m or lower (Grolander 2013).

2.1.1 Conceptual model

The purpose of the C14-SVAT model is to simulate the transport of C-14 that is released from the soil to the atmospheric layer closest to the soil surface. It is assumed in the model that C-14 will be fully mixed with stable carbon (C-12) in all atmospheric layers above the soil surface. The behaviour of C-14 in the atmosphere and the vegetation is likewise the behaviour of C-12, with only minor differences associated with isotopic effects, which are neglected in the model. Both C-14 and C-12 can be released from the soil to the canopy atmosphere either as CO_2 or methane. Releases in the form of methane will be dispersed in the atmosphere and will be not taken up by plants; unless methane is oxidized and changes into CO_2. At the same time, C-14 and C-12 that are present in the canopy atmosphere as CO_2 will be incorporated into plants by photosynthesis. In the C14-SVAT model it is conservatively assumed that C-14 is released to the canopy atmosphere as CO_2.

The C-14 that is released to air is transported vertically by turbulence and laterally with the advective flux of air, and steady-state conditions are assumed to occur on the time scale relevant to the safety assessment of disposal facilities (i.e. over a growing season or a year). The observed transport timescales are from seconds (in the canopy) to a few hours (in the soil), so the equilibrium assumption is well justified. Both isotopes (C-14 and C-12) are taken up by the vegetation from the canopy atmosphere by photosynthesis and released back to the canopy atmosphere by plant respiration. Both isotopes can also be taken up by the roots from the soil, where the C-14 to C-12 ration might be higher than in canopy atmosphere (Hoch 2014). The nature of the different processes involved and the assumption made for their modelling are discussed below.

Horizontal transport by advection

The C-14 that is present within and above the canopy atmosphere can be transported horizontally by advection in the direction of the wind, with fluxes that are proportional to the wind speed. Above the canopy, the wind speed increases with height, depending on the atmospheric conditions (stability) and it is also influenced by properties of the plants. Plants exert a frictional drag on moving air masses and thereby modify the local wind patterns. In the model, we assume a logarithmic wind profile, which is

commonly observed for the case of neutral stability conditions of the atmosphere. The justification for such approach is that, on average, daytime conditions in Sweden are close to neutral. For instance, the average daytime Monin Obukhov length at Norunda site (cf. Chapter 4) was about 800 m, which corresponds fairly well to neutral conditions. Also, in climatic modelling of micrometeorological conditions it is quite common to restrict stratification considerations to neutral conditions. For instance, Peinman-Monteith parameterization (Allen et al. 1998) of crop evapotranspiration on time scales of 10 days and longer is restricted to neutral conditions. The necessity of stability corrections arises only when this method is applied on shorter time scales.

For other stability conditions and short time scales, the impact from the canopy on the turbulence in the layers that are immediate above the canopy will also affect the wind profile (Tagesson 2012). However, as it will be shown in Chapter 4, for the time scales (season or year) that are relevant for the SR-PSU safety assessment, corrections of the wind profile for other stability conditions will have only negligible effects on the calculated daytime fluxes and activity concentrations in air. Therefore, stability corrections are not made in the C14-SVAT model, but only in the Lagrangian model presented in Chapter 3.

Generally, the wind speed in the canopy atmosphere also decreases downward towards the ground. There are, however, exceptions to this rule. For instance, in an open forest the air can "tunnel" under the branches and hence the wind speed can be greater there than further up in the plant community, where greater frictional drag occurs. So, air flow under plant communities also depends on the three-dimensional architecture of the plants. In the C14-SVAT model, the canopy layer of crops is considered homogeneous and an exponential decrease with height above ground of the wind speed is assumed.

Vertical transport by turbulence

C-14 released from the soil experiences vertical transport within and above the canopy atmosphere driven by turbulence. This transport process is commonly known as turbulent dispersion or Eddy diffusion. Random fluctuations in pressure in local regions of the turbulent air cause random motion of air packages, known as eddies, which move more or less as a unit, carrying with them large amounts of different gas molecules present in the atmosphere, such as H_2O vapour and CO_2. These eddies have a constantly changing shape and size, the latter being large compared with intermolecular distances. The eddying motions of the air packages promote a mixing, formally like the mixing due to molecular diffusion.

The intensity of the "diffusion" of air packages is described with the so-called Eddy Diffusion Coefficients (EDC), which unlike the ordinary diffusion coefficients have the same value in a given situation for all transported gas molecules. The EDC varies with wind speed within and above a plant canopy. The EDCs usually are approximately proportional to the local wind speed. As the wind speed increases, turbulent mixing of the air is more likely and thus the EDC becomes larger. Because wind speed varies with altitude and because EDC also depends on the gradient in the wind speed, averaged values of EDC over an appropriate distance are used to describe the vertical fluxes in some region of the turbulent air within and above the canopy. Moreover, the wind speed, its gradient, and the vertical temperature gradient all vary during the day. Consequently, EDC should also be averaged over a suitable time interval.

Near the ground the air is generally quite still and the EDC is low, often averaging 5×10^{-5} m^2/s over the first 10 mm above the ground (Nobel 2009), a value that is only about three times higher than the diffusion coefficient of CO_2 in air, 1.5×10^{-5} m^2/s (Lide 2008). When the EDC is of the same order of magnitude as diffusion coefficients, differences in movement among molecular species can become apparent. As we move upward to the top of a plant community, the EDC increases, often more or less logarithmically with height in the upper part of many plant communities (Tagesson 2012).

In the model it is assumed that the EDCs in different layers are constant in time and proportional to the wind speed. Their variation in height is dictated by the assumed wind profiles, which are the same that are assumed for modelling of advective transport (see above).

Transport by molecular diffusion

Molecular diffusion is a spontaneous process leading to the net movement of a substance from a region of higher concentration to an adjacent region of lower concentration of that substance. Diffusion in air is a result of the random thermal motion of the gas molecules in air. The net movement caused by diffusion is a statistical phenomenon, since a greater probability exists for molecules to move from the concentrated region to the dilute region than vice versa. Diffusion is involved in several processes of CO_2 transport in the soil-canopy atmosphere-plant system, such as gas exchange between the soil and the canopy atmosphere, and transport of CO_2 in the air surrounding and within the leaves, which is necessary for photosynthesis to take place. Molecular diffusion plays a limited role in the vertical transport within and above the canopy atmosphere, which is dominated by the vertical turbulent dispersion and is, therefore, not included explicitly in the C14-SVAT model.

Plant uptake by photosynthesis

Photosynthesis is the process by which organisms that contain the pigment chlorophyll convert light energy into chemical energy which can be stored in the molecular bonds of organic molecules. As a result of photosynthesis, C-14 that is released as CO_2 from the soil can be incorporated directly into plants. The rate of photosynthesis at each level of the plant canopy will depend on how the amount of light varies down through the various levels of vegetation. At each level of the plant community, the photosynthetic photon flux (PPF) consisting of wavelengths from 400 to 700 nm (Nobel 2009), helps determine the rate of photosynthesis there. As we move downward into the vegetation, the PPF decreases approximately exponentially due to absorption by the foliage. For some canopies the greatest leaf area per interval of height occurs near the middle (e.g. many grasses), and for others it occurs about three-fourths of the way up from the ground (e.g. many crops and trees). The PPF is attenuated down through the plant community in proportion to the leaf area index of the plant community and the so-called foliar absorption coefficient, which describes the sorption properties of a particular type of foliage. It should be noted that 2/3 or more of net photosynthesis usually occurs in the upper 1/3 of most plant communities (Nobel 2009).

Due to attenuation of the PPF, at a certain height in the canopy there is no net CO_2 uptake by a plant during day time, i.e. the net CO_2 flux is zero. This height is called the “light compensation point”. The light compensation point for leaves is approximately the same for C3 and C4 plants (Nobel 2009). Leaves shaded by many overlaying leaves can actually be at (or below) the light compensation point when exposed leaves have appreciable net rates of CO_2 uptake. Leaves that are below light compensation for most of the day do not contribute to the net photosynthesis of the plant. Such leaves generally loose from 50 % of their dry weight before dying and abscising.

In the C14-SVAT model, the uptake rate of C-14 from air by crops is modelled as a function of the gross primary production, which is proportional to the rate of photosynthesis. The process of photosynthesis and the variations in the photosynthesis rate with canopy height are not modelled explicitly.

Releases of C-14 to air by respiration and photorespiration

Respiration is the general process by which organisms oxidize organic molecules (e.g. sugars) and derive energy from the molecular bonds that are broken. Respiration in the roots cells and in soil microorganisms can lead to a net upward CO_2 flux density coming from the ground during the growing season (Nobel 2009). The CO_2 flux from the soil at night can be about half of the value at day time because of lower temperatures at night. Respiration averaged over a 24-hour period can be 20 % of gross photosynthesis for a rapidly growing plant community and can increase to over 50 % as the community matures. When considered over a growing season for a crop, respiration for an entire plant is from 30 to 50 % of gross photosynthesis (Nobel 2009).

Photorespiration is the uptake of O_2 and the evolution of CO_2 in the light resulting from glycolate synthesis in chloroplasts and subsequent glycolate and glycine metabolism in peroxisomes and mitocondria (Nobel 2009). Photorespiration has very low rates in C4 plants, but potential photosynthetic output may be reduced by photorespiration by up to 25 % in C3 plants (Sharkey 1988).

In the C14-SVAT model, respiration and photorespiration are not modelled explicitly, but are considered implicitly in the values of Net Primary Production used in the calculation of C-14 specific activities in primary producers.

Root uptake of C-14

Roots can directly incorporate inorganic carbon from the soil via root uptake. Estimates by Vuorinen et al. (1989) show that direct root uptake of carbon may be from 1 to 2 % of the carbon assimilated by leaves. At the same time, about 1–2 % of carbon that is assimilated by plants is released to the soil by root exudation (Kuzyakov and Domanski 2000). From a study using different types of soils, Sheppard et al. (1991) estimated that in carbonated soils about 1.7 % of the plant carbon may be derived directly from root uptake. The values were much lower in a non-carbonated soil. Amiro and Ewing, (1992) studied the uptake of inorganic C-14 by bean plant roots and showed that C-14 uptake via the roots was independent of the photosynthetic rate and, in most cases, could be predicted by knowing the transpiration rate and the nutrient solution concentration. However, when a less efficient root-medium aeration system was used, C-14 uptake was greater than predicted using transpiration (Amiro and Ewing 1992). It should be noted that the relative contribution of root uptake and assimilation by leaves to the total carbon incorporated by a plant could be different for C-12 and C-14; since the C-14 specific activities in the soil and canopy atmosphere could be different.

Root uptake is not included in the C14-SVAT model, but it is considered in the biosphere model used in the SR-PSU safety assessment. The fraction of carbon that is assimilated by root uptake is, however, taken into account in the calculation of fluxes from air to primary producers (see Section 2.1.5).

Compartments and processes included in the model

The C14-SVAT model includes three compartments corresponding to three atmospheric layers above the soil surface (Figure 2-1). The first atmospheric layer, the canopy layer (CA), extends from the soil surface to the top of the canopy of the vegetation. This is the layer where gas exchange between air and soil occurs, and where primary producers fix atmospheric carbon by photosynthesis. The second layer extends from the top of the canopy of the vegetation to 2.5 m above the ground. For vegetation with a canopy height lower than 1 m, the C-14 activity concentrations in this second layer can be used in estimations of inhalation doses to people present above a vegetated land. The third layer is required for representation of recycling of C-14 with turbulent transport. The effect of the assumed thickness of this layer on the model predictions is estimated in Chapter 5.

The C14-SVAT model can use as input C-14 releases to the canopy layer by degassing from the soil or by degassing of irrigation water intercepted by leaves.

The vertical arrows in Figure 2-1 represent the vertical transport by turbulence between the atmospheric layers. In the case of L2, turbulent transport back to this layer from upper layers is neglected, which is equivalent to assuming a boundary condition of zero C-14 concentration above this layer. Hence, the height of this layer should be taken sufficiently high for this assumption to hold. The horizontal arrows represent the C-14 transport by advection from each atmospheric layer.

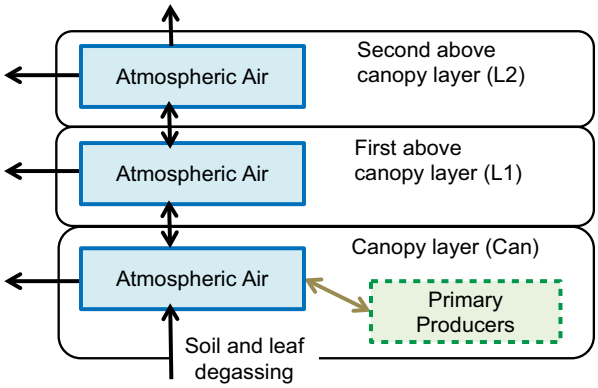

Figure 2-1. *A graphical representation of the model used to calculate the outcome of C-14 transport in the surface atmosphere above vegetated land. Boxes represent C-14 inventories and arrows fluxes of the C-14. Primary producers are assumed to be in steady state exchange with the atmospheric air of the canopy layer through photosynthesis and respiration (brown dashed arrow). The vertical and horizontal arrows represent C-14 fluxes driven by vertical turbulent and lateral advective air fluxes respectively (black arrows). Releases of C-14 to the canopy layer occurs by degassing from the soil and by degassing of irrigation water intercepted by leaves.*

For estimation of C-14 specific activity in plants the same approach as in Avila and Pröhl (2008) is used, consisting of assuming that the C-14 specific activity in primary producers is the same as the specific activity in air (the so-called specific activity approach). In the C14-SVATmodel, C-14 is treated as a tracer, i.e. changes in the C-14 air concentration profile caused by uptake of C-14 by plants via photosynthesis or releases by respiration are neglected. This assumption is also made for stable carbon and therefore the same concentration of stable carbon in air is used in the model for all atmosphere layers. The impact of treating C-14 and stable carbon as tracers is investigated in Chapter 5.

2.1.2 Mathematical model

The equations used in the C14-SVAT model for calculation of C-14 fluxes, concentrations and specific activities are presented in the following Sections 2.1.3 to 2.1.8). These equations have been derived from the solution for steady state conditions of a system of three ordinary differential equations (ODE). Each ODE represents the variation in time (t) of the C-14 inventory (Bq) in each of the three atmospheric layers included in the model, i.e. in the Canopy Layer (A_{CA}), the First Above-Canopy Layer (A_{L1}) and the Second Above-Canopy Layer (A_{L2}):

$$\frac{dA_{CA}}{dt} = ReleaseRate - Flux_{adv,CA} - Flux_{Turb,CAToL1} + Flux_{Turb,L1ToCA} - \frac{\left(1 - f_{rootUptake}\right)\cdot(GPP - R)}{conc_{C,atmos}\cdot height_{CA}} A_{CA} - \lambda . A_{CA}$$

$$\frac{dA_{L1}}{dt} = -Flux_{adv,L1} + Flux_{Turb,CAToL1} - Flux_{Turb,L1ToCA} + Flux_{Turb,L2ToL1} - Flux_{Turb,L1ToL2} - \lambda . A_{L1}$$

$$\frac{dA_{L2}}{dt} = -Flux_{adv,L2} + Flux_{Turb,L1To2} - Flux_{Turb,L2ToL1} - Flux_{Turb,L2ToOut} - \lambda . A_{L2}$$

where,

$ReleaseRate$ is the area normalized release rate of C-14 to the canopy layer [Bq m^{-2} y^{-1}],

$Flux_{adv,CA}$ is the area normalized flux of C-14 from the canopy layer by advective transport [Bq m^{-2} y^{-1}],

$Flux_{adv,L1}$ is the area normalized flux of C-14 from the L1 layer by advective transport [Bq m^{-2} y^{-1}],

$Flux_{adv,L2}$ is the area normalized flux of C-14 from the L2 layer by advective transport [Bq m^{-2} y^{-1}],

$Flux_{Turb,CAToL1}$ is the area normalized flux of C-14 from the canopy layer to the L1 layer by turbulent transport [Bq m^{-2} y^{-1}],

$Flux_{Turb,L1ToCA}$ is the area normalized flux of C-14 from the L1 layer to the canopy layer by turbulent transport [Bq m^{-2} y^{-1}],

$Flux_{Turb,L1ToL2}$ is the area normalized flux of C-14 from the L1 layer to the L2 layer by turbulent transport [Bq m^{-2} y^{-1}],

$Flux_{Turb,L2ToL1}$ is the area normalized flux of C-14 from the L2 layer to the L1 layer by turbulent transport [Bq m^{-2} y^{-1}],

$Flux_{Turb,L2ToOut}$ is the area normalized flux of C-14 from the L2 layer to upper layers by turbulent transport [Bq m^{-2} y^{-1}],

$f_{rootUptake}$ is the fraction of carbon assimilated via root uptake [kgC kgC^{-1}],

GPP is the gross primary production [kgC m^{-2} y^{-1}],

R is the autotrophic respiration rate [kgC m^{-2} y^{-1}],

$conc_{C,atmos}$ is the carbon concentration in the canopy layer [kgC m^{-3}],

$height_{CA}$ is the height above the ground of the upper boundary of the canopy layer [m],

λ is the C-14 radioactive decay constant [y^{-1}].

In steady state conditions, the C-14 inventory in each layer does not vary in time and the right hand side of each of the above ODEs can be set equal to zero. A system of linear equations was then obtained, which was solved algebraically to obtain the equations presented in the next sections. The radioactive decay of C-14 was neglected, since it is very long compared with the residence time of C-14 in the different compartments. The term (GPP-R) was substituted by the Net Primary Production (NPP), since values of NPP are usually easier to estimate. In the parameterization of the different transport processes the so-called method of resistances was applied, see Section 3.3.2, in a simplified way which allowed analytical solutions to be obtained. The potential effect of this simplification on the accuracy of the model predictions is studied in Chapter 5. Vertical advective fluxes were neglected since these are much smaller than the turbulent fluxes.

2.1.3 C-14 specific activity in the canopy layer

At steady state, the specific C-14 activity in canopy air can be obtained by dividing the C-14 flux from this compartment by the flux of stable carbon from the same compartment. Moreover, if radioactive decay of C-14 is neglected, then the C-14 flux from the canopy atmosphere will equal the net flux of C-14 into this compartment. Consequently, the C-14 specific activity in the canopy atmosphere, $SA^{14C}_{(atmos,can)}$ [BqkgC^{-1}], can be expressed as the ratio between the flux of C-14 into the canopy atmosphere and the flux of stable carbon out of the canopy atmosphere:

$$SA^{14C}_{atmos,can} = \frac{ReleaseRate}{Flux_{PP} + Flux_{turb} + Flux_{adv}} \quad \text{(Eq 2-1)}$$

where,

ReleaseRate is the area normalized release rate of C-14 to the canopy layer [Bq m^{-2} y^{-1}],

$Flux_{PP}$ is the area normalized net flux of stable carbon from the canopy air to the primary producers [kgC m^{-2} y^{-1}],

$Flux_{adv}$ is the area normalized net flux of stable carbon from the canopy air by advective transport [kgC m^{-2} y^{-1}], and

$Flux_{turb}$ is the area normalized net flux of stable carbon from the canopy air by turbulent transport [kgC m^{-2} y^{-1}].

2.1.4 Release of C-14 to the canopy layer

In this context, the release rate of C-14 into the canopy layer [Bq m^{-2} y^{-1}] consists of fluxes from *soil degassing*, including *litter respiration* and by degassing of irrigation water intercepted by plant leaves in cases in which the crops are irrigated with water contaminated with C-14. These fluxes represent inputs to the C14-SVAT model, which have to be estimated with other models.

2.1.5 Flux to primary producers

The net flux of stable carbon, $Flux_{PP}$ [kgC m^{-2} y^{-1}] to primary producers can be described with one equation for all terrestrial ecosystems:

$$Flux_{PP} = NPP \cdot (1 - f_{rootUptake}) \quad \text{(Eq 2-2)}$$

where,

NPP is the area-specific net primary production in ecosystem i [kgC m^{-2} y^{-1}], and

$f_{rootUptake}$ is the fraction of carbon assimilated via root uptake [kgC kgC^{-1}].

2.1.6 Turbulent flux

The area normalized net turbulent flux of carbon [kgC m^{-2} y^{-1}] from the canopy air is the product of the area specific turbulent upward flux of air and the carbon concentration in the atmospheric air, corrected for the downward turbulent back-flux of carbon. This flux is:

$$Flux_{turb} = \mathrm{Vel}_{\mathrm{exch,Ca,L1}} \cdot Conc_{C,atmos} \cdot (1 - RF_{L1ToCA}) \qquad \text{(Eq 2-3)}$$

where,

$Conc_{C,atmos}$ is the carbon concentration in atmospheric air [kgC m^{-3}],

$Vel_{exch,Ca,L1}$ is the velocity of air exchange between the canopy and first above canopy layer by turbulent transport [m y^{-1}], and

RF_{L1ToCA} is the carbon recycling factor from the first above-canopy layer to the canopy layer [unitless].

The carbon that enters the first above-canopy layer (L1), from the canopy layer, can be transported laterally with the advective flux of air, vertically to the second above-canopy layer or recycled back to the canopy layer by turbulent transport. The fraction that is transported by a specific pathway will depend on the relative magnitude of the air exchange velocity of this pathway, as compared with other competing pathways. The recycled fraction (RF) is calculated as the ratio of the velocity of air exchange between the canopy and first above-canopy layer and the total velocity of air exchange in the first above-canopy layer (Equation 2-4). This ratio corresponds to the probability that a molecule of stable carbon (and also C-14) released from the canopy layer to the first above-canopy layer, will be recycled back to the canopy layer.

$$\mathrm{RF_{L1ToCA}} = \frac{\mathrm{Vel_{exch,CA,L1}}}{\mathrm{Vel_{exch,L1,L2}}(1 - \mathrm{RF_{L2ToL1}}) + \mathrm{Vel_{exch,CA,L1}} + \mathrm{Vel_{Adv,L1}}} \qquad \text{(Eq 2-4)}$$

where,

$Vel_{exch,Ca,L1}$ is the velocity of air exchange between the canopy and first above canopy layer by turbulent transport [m y^{-1}],

$Vel_{exch,L1,L2}$ is the velocity of air exchange between the first and second above-canopy layers by turbulent transport [m y^{-1}],

$Vel_{Adv,L1}$ is the air exchange velocity of the first canopy layer by advective transport [m y^{-1}] (see below), and

RF_{L2ToL1} is the carbon recycling factor from the second above-canopy layer to the first above-canopy layer [unitless].

The Recycling Factor from the second (L2) to the first (L1) above-canopy layer is calculated similarly (see Equation 2-5). However, in this case, the recycling from the uppermost layer to the second above-canopy layer has been neglected for simplicity. This is justified by the fact that concentrations in air of stable carbon (and C-14) originated from the canopy layer substantially decrease with the height above canopy. As shown in Chapter 3, this simplification does not lead to a significant underestimation of the Recycling Factor.

$$\mathrm{RF_{L2ToL1}} = \frac{\mathrm{Vel_{exch,L1,L2}}}{\mathrm{Vel_{exch,L2,Upp}} + \mathrm{Vel_{exch,L1,L2}} + \mathrm{Vel_{Adv,L2}}} \qquad \text{(Eq 2-5)}$$

where,

$Vel_{exch,L2,Upp}$ is the velocity of air exchange between the second above canopy layer and upper layers of the atmosphere by turbulent transport [m y^{-1}], and

$Vel_{Adv,L2}$ is the air exchange velocity of the second canopy layer by advective transport [m y^{-1}].

The upward turbulent exchange velocities, Vel_{exch} [m y^{-1}], are calculated as the inverse of the average resistances of two adjacent layers, which follows from the definition of resistance (see below). For simplicity, the resistance of the uppermost layer (above the second above-canopy layer) has been neglected. This simplification is justified by the fact that the resistance decreases substantially with height and, as shown in Chapter 5, this simplification does not lead to significant overestimation of the exchange rates. The equations used for calculating the exchange velocities are:

$$\mathrm{Vel_{exch,CA,L1}} = \frac{1}{0.5(res_{CA} + res_{L1})} \qquad \text{(Eq 2-6)}$$

$$\mathrm{Vel_{exch,L1,L2}} = \frac{1}{0.5(res_{L1} + res_{L2})} \qquad \text{(Eq 2-7)}$$

$$\mathrm{Vel_{exch,L2,Upp}} = \frac{1}{0.5 \cdot res_{L2}} \qquad \text{(Eq 2-8)}$$

where,

res_{CA} is the resistance of the canopy layer to turbulent transport [y m^{-1}],

res_{L1} is the resistance of the first above-canopy layer to turbulent transport [y m^{-1}], and

res_{L2} is the resistance of the second above-canopy layer to turbulent transport [y m^{-1}].

The resistance to turbulent transport, *res* [y m^{-1}], of an atmospheric layer is defined as the ratio between the thickness and the eddy diffusion coefficient of the layer (Wilson 1989, Wilson and Sawford 1996, Finnigan 2000, Baldocchi et al. 1983, Shuttleworth and Wallace 1985, Shuttleworth and Gurney 1990):

$$\mathrm{res_{CA}} = \frac{z_{CA}}{D_{CA}} \qquad \mathrm{res_{L1}} = \frac{z_{L1}}{D_{L1}} \qquad \mathrm{res_{L2}} = \frac{z_{L2}}{D_{L2}} \qquad \text{(Eq 2-9)}$$

where,

z is the thickness of the atmospheric layer (canopy, first and second above the canopy) [m], and

D is the eddy diffusion coefficient of corresponding layer [m^2 y^{-1}].

For the above canopy layers (L1 and L2), we assume that the eddy diffusion coefficient at a given height above the ground (*h*) is proportional to the height above the displacement plane ($height_{displ}$), i.e. to ($h - height_{displ}$). Under this assumption the eddy diffusion coefficients, *D* [m^2 y^{-1}], for these layers become:

$$\mathrm{D_{L1}} = \frac{Karman_{const} \cdot Vel_{frict} \cdot z_{L1}}{ln\left(\frac{height_{L1} - height_{displ}}{height_{CA} - height_{displ}}\right)}$$

$$\mathrm{D_{L2}} = \frac{Karman_{const} \cdot Vel_{frict} \cdot z_{L2}}{ln\left(\frac{height_{L2} - height_{displ}}{height_{L1} - height_{displ}}\right)} \qquad \text{(Eq 2-10)}$$

where,

$$height_{displ} = 0.75 \cdot height_{CA}$$

$Karman_{const}$ is the von Karman constant [unitless],

Vel_{frict} is the friction velocity [m y^{-1}],

$height_{CA/L1/L2}$ is the height above the ground of the upper boundary of the canopy, the L1 and the L2 layers, respectively [m], and

$height_{displ}$ is the height of the displacement plane assumed to be 75 % of the canopy height [m].

The displacement plane is the height above the surface where the wind speed is taken to fall to zero. This is assumed to lie within the canopy. The friction velocity (also called shear velocity) is a convenient way of defining a velocity scale close to a surface, by which the shear stress may be re-written in units of velocity. The friction velocity is calculated from the wind speed at reference height, assuming that the wind speed increases logarithmically with height:

$$Vel_{frict} = \frac{Karman_{const} \cdot Vel_{wind,heigh,ref,ter}}{ln\left(\frac{height_{ref,ter} - height_{displ}}{z_0}\right)} \qquad \text{(Eq 2-11)}$$

$$z_0 = 0.1 \cdot height_{CA}$$

where,

$Vel_{wind,heigh,ref,ter}$ is the wind speed at the reference height $height_{ref,ter}$ [m y^{-1}],

$height_{ref,ter}$ is the reference height [m], and

z_0 is the roughness length, assumed to be 10 % of the canopy height [m].

More rigorously, Equation 2-10 should only be used for above-canopy layers in neutral atmospheric stability conditions. For other stability conditions and short time scales, it is necessary to account for the impact from the canopy on the turbulence in the layers that are immediately above the canopy (Tagesson 2012). However, for the time scales of relevance for this safety assessment (seasonal or annual) corrections for other stability conditions have negligible effects on the calculated turbulent fluxes and activity concentrations in the air (see Chapter 4).

Nevertheless, using Equation 2-10 for the canopy layer would lead to overestimation of the eddy diffusion coefficients and the turbulent upward fluxes of air. Instead, an exponential dependency of the eddy diffusion coefficients with height is commonly assumed (Shuttleworth and Gurney 1990). With an exponential dependency, the eddy diffusion coefficient of the canopy layer, D_{CA} [m^2 y^{-1}], becomes:

$$\mathrm{D_{CA}} = \frac{D(z_{CA}) \cdot Coeff_{ext}}{e^{Coeff_{ext}} - 1}$$

$$D(z_{CA}) = Karman_{const} \cdot Vel_{frict} \cdot (z_{CA} - height_{displ}) \qquad \text{(Eq 2-12)}$$

where,

$D(z_{CA})$ is the eddy diffusion coefficient at the canopy height [m^2 y^{-1}], and

$Coeff_{ext}$ is the extinction coefficient [unitless].

The extinction coefficient, $Coeff_{ext}$ [unitless], determinates the rate of decrease of the eddy diffusion coefficient with height in the canopy. It is calculated from canopy properties such as the leaf drag and the mixing length inside the canopy (Kustas 1990):

$$\mathrm{Coeff_{ext}} = \sqrt{\frac{dragCoef \cdot LAI \cdot z_{CA}}{L_m}} \qquad \mathrm{L_m} = \sqrt{\frac{4 \cdot leaf_{width} \cdot z_{CA}}{\pi \cdot LAI}} \qquad \text{(Eq 2-13)}$$

where,

$dragCoef$ is the drag coefficient of the canopy [unitless],

LAI is the leaf area index of the canopy of mire vegetation or cultivated species [m^2 m^{-2}],

L_m is the mean mixing length inside the canopy [m], and $leaf_{width}$ is the leaf width of mire-canopy-forming vegetation or cultivated species [m].

The approach adopted for calculation of the eddy diffusion coefficient at the canopy height (Equation 2-12) has the implicit assumption that there is continuity of the diffusion coefficient at the border between the above canopy and canopy layers. However, it is known that turbulence at the top of the canopy is greatly increased and therefore a discontinuous profile of the eddy diffusion coefficient might be more appropriate. The effect on the predictions of the profile of C-14 concentrations of the assumptions about the continuity of the eddy diffusion coefficient is further discussed in Chapter 5.

2.1.7 Advective flux

The recycling to the canopy air of C-12 (and C-14) that is laterally transported from this layer by advection can be neglected, because substantial dilution takes place downstream. Hence, the total flux of carbon by advective transport can be used in Equation 2-1, instead of the net flux. The area specific total advective flux of carbon from the canopy layer, $Flux_{adv}$ [kgC m^{-2} y^{-1}], is the product of the area-specific horizontal advective flux of air and the concentration of stable carbon in the canopy air:

$$Flux_{adv} = \mathrm{Vel}_{\mathrm{Adv,CA}} \cdot conc_{C,atmos} \qquad \text{(Eq 2-14)}$$

where,

$conc_{C,atmos}$ is the carbon concentration in the canopy layer [kgC m^{-3}], and

$Vel_{Adv,CA}$ is the air-exchange velocity of the canopy layer by advective transport [m y^{-1}].

The advective air-exchange velocity is defined as the advective flux of air through a plane perpendicular to the main wind direction, normalized by the area of the object. To parameterise the exchange velocity, the atmospheric layers are represented for simplicity as a cube with an area equal to the area of the object that receives the releases and a height equal to the thickness of the corresponding atmospheric layer. Usage of a circular area, instead of a cube, might be more appropriate. However, this does not lead to significant difference in the calculated values of the air-exchange velocity. For the assumed geometry, the advective exchange velocities, Vel_{Adv} [m y^{-1}], of the different layers (Canopy, L1 and L2) can be calculated with the following equation:

$$\mathrm{Vel}_{\mathrm{Adv}} = \frac{Vel_{wind} \cdot z}{\sqrt{area}} \qquad \text{(Eq 2-15)}$$

where,

Vel_{wind} is the average wind speed in the corresponding atmospheric layer [m y^{-1}],

$area$ is the surface area of the vegetated land receiving the C-14 releases [m^2],

z is the thickness of the corresponding atmospheric layer [m].

For the above canopy layers (L1 and L2) the wind speed is assumed to increase as a logarithmic function of height above the displacement plane (HAD). Thus the average wind speed in these layers can be expressed as:

$$Vel_{wind,L1} = \frac{Vel_{frict}}{Karman_{const}}\left(\left(\frac{HAD_{L1}}{z_{L1}}\right)\left(\ln\left(\frac{HAD_{L1}}{z_0}\right)-1\right)-\left(\frac{HAD_{CA}}{z_{L1}}\right)\left(\ln\left(\frac{HAD_{CA}}{z_0}\right)-1\right)\right)$$

$$HAD_{CA} = height_{CA} - height_{displ} \qquad HAD_{L1} = height_{L1} - height_{displ}$$

$$Vel_{wind,L2} = \frac{Vel_{frict}}{Karman_{const}}\left(\left(\frac{HAD_{L2}}{z_{L2}}\right)\left(\ln\left(\frac{HAD_{L2}}{z_0}\right)-1\right)-\left(\frac{HAD_{L1}}{z_{L2}}\right)\left(\ln\left(\frac{HAD_{L1}}{z_0}\right)-1\right)\right) \qquad \text{(Eq 2-16)}$$

$$HAD_{L2} = height_{L2} - height_{displ}$$

$$height_{displ} = 0.75 \cdot height_{CA} \qquad z_0 = 0.1 \cdot height_{CA}$$

where,

$Karman_{const}$ is the von Karman constant [unitless],

Vel_{frict} is the friction velocity [m y^{-1}],

$height_{CA/L1/L2}$ is the height above the ground of the upper boundary of the canopy, the L1 and the L2 layers, respectively [m],

$height_{displ}$ is the height of the displacement plane assumed to be 75 % of the canopy height [m],

z is the thickness of an atmospheric layer (canopy, first and second above the canopy) [m],

z_0 is the roughness length, assumed to be 10 % of the canopy height [m].

For the canopy layer (CA) the wind speed is assumed to increase as an exponential function of height above the ground (Shutleworth and Gurney 1990). Thus the average wind speed in the layer can be calculated as:

$$Vel_{wind,CA} = Vel_{wind}(z_{CA})\frac{1 - e^{-Coeff_{ext}}}{Coeff_{ext}} \quad \text{(Eq 2-17)}$$

where,

$Vel_{wind}(z_{CA})$ is the wind speed at the canopy height [m y^{-1}], and

$Coeff_{ext}$ is the extinction coefficient [unitless] (see Equation 2-13).

From the logarithmic wind profile above the displacement plane, assumed for the above-canopy layers, the wind speed at the canopy height can be calculated as:

$$Vel_{wind}(z_{CA}) = \frac{Vel_{frict}}{Karman_{const}} \cdot ln\left(\frac{z_{CA} - height_{displ}}{z_0}\right) \quad \text{(Eq 2-18)}$$

2.1.8 Activity concentrations

The main output of the atmosphere sub-model is the C-14 specific activity in the canopy atmosphere (Equation 2-1), which is used to calculate plant uptake and the activity concentration in crop biomass. For this, the specific activity of the newly created biomass is assumed to equal the specific activity in the canopy atmosphere (Avila and Pröhl 2008). In addition, the C-14 activity concentration in air is calculated, which is used to estimate exposure from inhalation. For ecosystems with a canopy height above 2 m, the activity concentration in the canopy air can be used to calculate inhalation doses. However, as cultivated crops have a limited height (< 1m), the activity concentration in the first above-canopy layer is used for this purpose. The C-14 activity concentration in atmospheric air, $AC^{14C}_{atmos,CA}$ [Bq m^{-3}] of the canopy layer is calculated as:

$$AC^{14C}_{atmos,CA} = SA^{14C}_{atmos,can} \cdot Conc_{C,atmos} \quad \text{(Eq 2-19)}$$

where,

$SA^{14C}_{atmos,can}$ the C-14 specific activity in the canopy atmosphere, [Bq kgC^{-1}],

$Conc_{C,atmos}$ is the carbon concentration in air [kgC m^{-3}].

In this assessment, the same value of carbon concentration in air has been used in Equations 2-3 and 2-19. More rigorously, in Equation 2-3 the value corresponding to the first above-canopy layer should have been used and in Equation 2-19 the value for the canopy layer would have been more appropriate. However, the difference between these values is negligible for this assessment context (see Chapter 5) and, for this reason; a general value of carbon concentration in air has been used in both equations.

The area normalized C-14 flux from the canopy layer to the first above-canopy layer equals the C-14 activity concentration in the canopy air (Equation 2-19) times the velocity or air exchange between these layers, which is the numerator in Equation 2-4. At the same time, the total area normalized C-14 flux from the first above-canopy layer equals the C-14 activity concentration in this layer times the total velocity of air exchange of this layer, which is the denominator in Equation 2-5. At steady state, these two fluxes equal each other. From these considerations, the following equation for the C-14 activity concentration in the atmospheric air of the first above-canopy layer is obtained:

$$AC^{14C}_{atmos,L1} = AC^{14C}_{atmos,CA} \cdot RF_{L1ToCA} \qquad \text{(Eq 2-20)}$$

where,

RF_{L1ToCA} is the carbon recycling factor from the first above-canopy layer to the canopy layer [unitless].

2.2 Surface atmosphere above water bodies

The conceptual model of the near-surface atmosphere above water bodies includes two atmospheric layers and is similar to the model presented in Figure 2-1, but without the canopy layer. C-14 is released to the layer closest to the water surface (see below), and it is assumed that C-14 will be fully mixed with stable carbon (C-12) in all atmosphere layers. Both isotopes are transported vertically by turbulence and laterally with the advective flux of air, and steady-state conditions are assumed to apply at the time scale relevant for the safety assessment (i.e. over a year). The target endpoint of the model is the C-14 activity concentration in atmospheric air, used in the calculation of the reverse C-14 flux from the atmosphere to the surface water.

The first atmospheric layer, the L1 layer, extends from the water surface to a height of 1 m. This is the layer where gas exchange between air and water occurs. The second layer is required for representation of recycling of C-14 with turbulent transport. The assumed thickness of this layer has only a slight impact on the prediction of the target endpoint.

2.2.1 Activity concentrations in atmospheric air

The C-14 activity concentration in the first layer, L1, can be obtained by dividing the area normalized release of C-14 into this layer by the total velocity of air exchange of this layer, including the net air exchange with the second layer, L2 by turbulent transport and the lateral air exchange by advective transport:

$$AC^{14C}_{atmos,L1} = \frac{ReleaseRate}{\mathrm{Vel}_{\mathrm{exch,L1,L2}}(1 - \mathrm{RF}_{\mathrm{L2ToL1}}) + \mathrm{Vel}_{\mathrm{Adv,L1}}} \qquad \text{(Eq 2-21)}$$

where,

ReleaseRate is the area normalized release rate of C-14 from the water to the L1 layer [Bq m^{-2} y^{-1}],

$Vel_{exch,L1,L2}$ is the velocity of air exchange between the first, L1, and second, L2, layers by turbulent transport [m y^{-1}],

$Vel_{Adv,L1}$ is the air exchange velocity of the L1 layer by advective transport [m y^{-1}], and

RF_{L2ToL1} is the air recycling factor from the second layer to the first layer by turbulent transport [unitless].

2.2.2 Turbulent fluxes

The equation for the Recycling Factor, RF [unitless], from L2 to L1 is the same equation which is presented in Section 2.1.6 for the surface atmosphere above vegetated land:

$$\mathrm{RF}_{\mathrm{L2ToL1}} = \frac{\mathrm{Vel}_{\mathrm{exch,L1,L2}}}{\mathrm{Vel}_{\mathrm{exch,L2,Upp}} + \mathrm{Vel}_{\mathrm{exch,L1,L2}} + \mathrm{Vel}_{\mathrm{Adv,L2}}} \qquad \text{(Eq 2-22)}$$

where,

$Vel_{exch,L1,L2}$ is the velocity of air exchange between the first and second layers by turbulent transport [m y^{-1}],

$Vel_{exch,L2,Upp}$ is the velocity of air exchange between the second and upper layers of the atmosphere by turbulent transport [m y^{-1}],

$Vel_{Adv,L2}$ is the air exchange velocity of the second layer by advective transport [m y^{-1}].

The upward turbulent exchange velocities, Vel_{exch} [m y^{-1}], are calculated as the inverse of the average resistance of the two adjacent layers, which follows from the definition of resistance (see Section 2.1.6). For simplicity, the resistance of the uppermost layer (above L2) has been neglected. This simplification is justified by the fact that the resistance decreases substantially with height and, as shown in Chapter 5, this simplification does not lead to significant overestimation of the exchange rates. The equations used for calculating the exchange velocities are:

$$\mathrm{Vel_{exch,L1,L2}} = \frac{1}{0.5(res_{L1} + res_{L2})} \qquad \text{(Eq 2-23)}$$

$$\mathrm{Vel_{exch,L2,Upp}} = \frac{1}{0.5 \cdot res_{L2}} \qquad \text{(Eq 2-24)}$$

where,

res_{L1} is the resistance of the first layer to turbulent transport [y m^{-1}], and

res_{L2} is the resistance of the second layer to turbulent transport [y m^{-1}].

The resistance to turbulent transport, res [y m^{-1}], of an atmospheric layer is defined in the same way as in Section 2.1.6:

$$\mathrm{res_{L1}} = \frac{z_{L1}}{D_{L1}} \qquad \mathrm{res_{L2}} = \frac{z_{L2}}{D_{L2}} \qquad \text{(Eq 2-25)}$$

where,

z is the thickness of an atmospheric layer (first and second above the canopy) [m], and

D is the eddy diffusion coefficient of corresponding layer [m^2 y^{-1}],

For both layers (L1 and L2), we assume that the eddy diffusion coefficient is proportional to the height above the water. Under this assumption, the eddy diffusion coefficients, D [m^2 y^{-1}], for these layers become:

$$\mathrm{D_{L1}} = \frac{Karman_{const} \cdot Vel_{frict} \cdot z_{L1}}{ln\left(\frac{z_{L1}}{z_0}\right)} \qquad \text{(Eq 2-26)}$$

$$\mathrm{D_{L2}} = \frac{Karman_{const} \cdot Vel_{frict} \cdot z_{L2}}{ln\left(\frac{z_{L1} + z_{L2}}{z_{L1}}\right)}$$

where,

$Karman_{const}$ is the von Karman constant [unitless],

Vel_{frict} is the friction velocity [m y^{-1}], and

z_0 is the roughness length [m].

The friction velocity, Vel_{frict} [m y^{-1}], is calculated from the wind speed at a reference height, assuming that the wind speed increases logarithmically with height:

$$Vel_{frict} = \frac{Karman_{const} \cdot Vel_{wind,heigh,ref,ter}}{ln\left(\frac{height_{ref,ter}}{z_0}\right)} \qquad \text{(Eq 2-27)}$$

$$z_0 = 0.1 \cdot height_{CA}$$

where,

$Vel_{wind,heigh,ref,ter}$ is the wind speed reference height $height_{ref,ter}$ [m y^{-1}], and

$height_{ref,ter}$ is the reference height [m].

2.2.3 Advective fluxes

The advective fluxes, Vel_{Adv} [m y^{-1}], from the L1 and L2 layers are defined and calculated in the same way as in Section 2.1.7, with the following equation:

$$\mathrm{Vel_{Adv,i}} = \frac{Vel_{wind,i} \cdot z_i}{\sqrt{area}} \qquad i = \{L1, L2\} \qquad \text{(Eq 2-28)}$$

where,

Vel_{wind} is the average wind speed in the two atmospheric layers [m y^{-1}],

z is the thickness of the *L1* and *L2* layers [m],

$area$ is the surface area of water body [m^2], and

i is the index for the first and second layers.

For the L1 and L2 layers, the wind speed is assumed to increase as a logarithmic function of height. Thus, the average wind speed in these layers, Vel_{wind} [m y^{-1}] can be expressed as:

$$Vel_{wind,L1} = \frac{Vel_{frict}}{Karman_{const}}\left(\left(\ln\left(\frac{z_{L1}}{z_0}\right) - 1\right) + \frac{z_0}{z_{L1}}\right)$$

$$Vel_{wind,L2} = \frac{Vel_{frict}}{Karman_{const}}\left(\left(\frac{z_{L1}+z_{L2}}{z_{L2}}\right)\left(\ln\left(\frac{z_{L1}+z_{L2}}{z_0}\right) - 1\right) - \left(\frac{z_{L1}}{z_{L2}}\right)\left(\ln\left(\frac{z_{L1}}{z_0}\right) - 1\right)\right) \qquad \text{(Eq 2-29)}$$

where,

Vel_{frict} is the friction velocity [m y^{-1}] (see Equation 2-11),

$Karman_{const}$ is the von Karman constant [unitless],

z is the thickness of the L1 and L2 layers [m], and

z_0 is the roughness length [m].

3 Lagrangian model of turbulent transport

One difficulty in modelling of C-14 dispersion in the atmosphere in presence of plant canopies is the parameterization of the turbulent exchange processes. This difficulty arises from the fact that in the so-called roughness sub-layer (RSL) – inside and above canopy, up to a height of approximately 3 times the height of the canopy, the well-known similarity relationships (which are usually valid in the atmospheric surface layer up to heights of about 50–200 m) are violated.

Up to now, several approaches of different levels of complexity have been developed to account for the influence of RSL on turbulent transport. The most widely adopted approaches are: 1) modifications of the turbulent diffusion coefficient using various parameterizations of turbulence inside the canopy; 2) the so-called Linearized Near-Field Theory (LNF) developed by Raupach (1989) on the basis of the Lagrangian principles, which to some extent accounts for the non-local nature of turbulence inside the canopy; and 3) more comprehensive and computationally demanding higher-order turbulence closure schemes.

The first approach has been implemented in the C14-SVAT model described in Chapter 2, although in a simplified way. In this chapter, we describe the implementation of a model based on the second approach, which hereafter will be called the Lagrangian model. This model is based on the LNF theory as described in Harman and Finnigan (2008) (which will be further referenced here as HF08), where a gradient parameterization of turbulent momentum and concentration fluxes above a 'deep' canopy was proposed. The HF08 parameterization takes into account the influence of the RSL on the vertical distribution of the turbulent diffusion and viscosity coefficients. In HF08, the correction functions used in the parameterization were derived analytically by fitting velocity and concentration profiles inside and above the canopy. The profiles inside the canopy are obtained by using the assumption of constant mixing length. At present, HF08 is the most state-of-art parameterization of turbulent diffusion coefficients in the presence of a plant canopy.

The model equations of the Lagrangian model are presented in Chapter 3.1 using the nomenclature presented in Appendix 1. The parameterization proposed in HF08, and used in the Lagrangian model, is presented in Section 3.2 and finally the methods used for solution of the model equations are presented in Sections 3.3 and 3.4.

3.1 Model equations

The Lagrangian model developed in this work considers the case of a horizontally homogeneous canopy covering a flat terrain and assumes constant and homogeneous meteorological conditions. The area of the canopy is sufficiently large, so that lateral advective fluxes in the central part of the canopy can be neglected, since they are compensated. Thus, ignoring advective fluxes, a simple one-dimensional model describing the turbulent transport with the following equations for the concentrations of CO_2 ($C(z)$) and of $^{14}CO_2$ ($C^{14}(z)$) can be used:

$$-dK_c\left(dC/dz\right)/dz = S_R\left(z\right) - S_P\left(z\right) \qquad \text{(Eq 3-1)}$$

$$-dK_c\left(dC^{14}/dz\right)/dz = -\left(\frac{C^{14}\left(z\right)}{C\left(z\right)}\right)S_P\left(z\right) \qquad \text{(Eq 3-2)}$$

Here $S_R(z)$, $S_P(z)$ are source rates (per unit volume) of CO_2 due to respiration and photosynthesis respectively. The respiration rate is not included in right hand side of Equation 3-2, since it is assumed that all C-14 comes from ground, which is taken into account in the boundary conditions. The boundary conditions at the reference height H are assumed to be known:

$$C\big|_{z=z_r} = C_r\,,\; C^{14}\big|_{z=z_r} = 0 \qquad \text{(Eq 3-3)}$$

The fluxes of CO_2 and C-14 at the ground surface are assumed to be known:

$$-K_c\left(dC/dz\right)\Big|_{z=0} = R_0 \qquad \text{(Eq 3-4)}$$

$$-K_c\left(dC^{14}/dz\right)\Big|_{z=0} = Q_S \qquad \text{(Eq 3-5)}$$

The flux of $^{14}CO_2$ at the ground surface (Q_s) may be related to the respiration flux at the ground surface R_0, i.e. it may be a certain fraction of R_0, or it may be an independent parameter.

Alternative forms of Equations 3-1 to 3-5 are the equations for fluxes, which will be also used further here:

$$-K_c\left(dC/dz\right) = R_0 + \int_0^z \left(S_R\left(z\right) - S_P\left(z\right)\right)dz = R\left(z\right) - P\left(z\right) \qquad \text{(Eq 3-6)}$$

$$-K_c\left(dC^{14}/dz\right) = Q_s - \int_0^z \left(\frac{C^{14}\left(z\right)}{C\left(z\right)}\right) S_P\left(z\right)dz \approx Q_s - \frac{1}{C_r}\int_0^z C^{14}\left(z\right) S_P\left(z\right)dz = Q\left(z\right) \qquad \text{(Eq 3-7)}$$

The $1/C(z)$ in the right hand side of Equation 3-7 has been substituted with $1/C_r$, based on the fact that normally: $|(C(z) - C_r)/C_r| \ll 1$.

The relationships in HF08 are used to define the vertical profiles of K_c (z). Alternatively, inside the canopy turbulent diffusivity profiles can be parameterized using empirical relationships found in literature, as described below.

3.2 Relationships used in HF08 for the diffusion coefficient

In Belcher et al. (2012), Harman and Fiinnigan (2007) and HF08 a theory has been developed that takes into account the influence of the roughness sub-layer on the turbulent exchange of momentum and scalars above a deep canopy. Below we review in brief the main relationships used in HF08 and the assumptions made therein. However, some of the notation is changed as compared to HF08, where this was found to be convenient for the purposes of the present study. In particular, we choose a coordinate origin at the ground and not at the canopy height as is the case in HF08. The reason is that HF08 considers the asymptotic case of an infinitely deep canopy and therefore the canopy height does not influence the vertical profiles of velocities and concentrations. In our practical case, the canopy depth is finite and therefore the canopy height is an important parameter.

Following Garratt (1980), the common relationship for the vertical turbulent exchange coefficient of momentum and scalar quantities (such as humidity, temperature and contaminant's concentration) in the inertial above-canopy sub-layer of the surface layer is modified to account for the influence of the roughness sub-layer on turbulence exchange:

$$K_{m(c)} = \frac{\kappa u_*\left(z-d\right)}{\Phi_{m(c)}} = \frac{\kappa u_*\left(z-d\right)}{\varphi_{m(c)}\left(\left(z-d\right)/L\right)\hat{\varphi}_{m(c)}\left(\left(z-d\right)/z_*\right)} \qquad \text{(Eq 3-8)}$$

The stability correction functions $\varphi_{m(c)}$ have been widely studied (see Arya 2001 for a review). In several works, correction functions accounting for the roughness sub-layer influence $\hat{\varphi}_{m(c)}$ have been parameterized by using empirical relationships (e.g. Garratt 1980, Mölder et al. 1999). In HF08, the relationships for $\hat{\varphi}_{m(c)}$ are derived by matching inside- and above-canopy distributions at the canopy height, under the assumptions listed below.

In HF08, the canopy is considered to be sufficiently deep, i.e. all momentum drag is produced by canopy elements and not by the underlying soil. Thus, the lower boundary condition for the momentum is: $q_m|_{z=-\infty} = 0$. The mixing-length turbulence closure is used both inside and above the canopy, according to which turbulent momentum and concentration fluxes are expressed using

mixing lengths l_m and $l_c = l_m/S_c$ as: $\langle u'w' \rangle = -l_m^2 (dU/dz)^2$, $\langle C'w' \rangle = -l_m l_c \mid dU/dz \mid (dC/dz)$. Length scales $l_{m(c)}$, frontal leaf area per unit volume a and turbulent Schmidt number are taken to be constant inside the canopy. Stability effects are taken into account only above the canopy. Taking into account the listed assumptions, wind and scalar profiles inside the canopy are controlled by the following parameters: velocity U_h at canopy height and concentration C_0 at foliage surface; ratio of friction velocity u_* to reference wind velocity at canopy height U_h: $\beta = u_*/U_h$; length scale L_c depending on the drag coefficient at the leaf level c_d, and frontal leaf area per unit volume a: $L_c = 1/(c_d a)$; the leaf-level Stanton number r and momentum transfer to the leaf; the Schmidt number inside canopy: $S_{cc} = K_m/K_c|_{z<h} = S_c|_{z<h}$.

Using the above assumptions, the velocity profile inside the canopy is obtained:

$$U(z) = U_h \exp\left(\beta (z-h)/l_m\right) \qquad \text{(Eq 3-9)}$$

$l_m = 2\beta^3 L_c = 2\beta^3/(c_d a)$, which results in the following relationship for the turbulent diffusion coefficient inside the canopy:

$$\begin{aligned} K_c &= l_m l_c \left(dU/dz\right) = \frac{l_m^2}{S_{cc}} \frac{U_h \beta}{l_m} \exp\left(\frac{\beta(\mathrm{z-h})}{l_m}\right) = \\ &= \frac{l_m U_h \beta}{S_{cc}} \exp\left(\frac{\beta(\mathrm{z-h})}{2\beta^3 L_c}\right) = \frac{2\beta^3 L_c u_*}{S_{cc}} \exp\left(\frac{z-h}{2\beta^2 L_c}\right), \quad z < h \end{aligned} \qquad \text{(Eq 3-10)}$$

It is then assumed in HF08 that the length scale relevant to the depth of the roughness sub-layer is the 'vorticity thickness' $U/(dU/dz) = l_m/\beta$ and hence the following relationship for $\hat{\varphi}_{m(c)}$ is proposed:

$$\hat{\varphi}_{m(c)} = 1 - c_{m(c)} \exp\left\{-c_{2m(c)} \beta (z-d)/l_m\right\} \qquad \text{(Eq 3-11)}$$

The relationships for $c_{m(c)}$ are obtained from the continuity of momentum and scalar at the canopy top, as well as from the continuity of their fluxes and second derivatives:

$$c_m = \left[1 - \frac{\kappa}{2\beta\phi_m(z=h)}\right] \exp(c_{2m}/2) \qquad \text{(Eq 3-12)}$$

$$c_c = \left[1 - \frac{\kappa S_{cc}}{2\beta\phi_c(z=h)}\right] \exp(c_{2c}/2) \qquad \text{(Eq 3-13)}$$

$$c_{2m} = \kappa \left(3 - \frac{2\beta^2 L_c}{\varphi_m(z=h)} \left.\frac{d\varphi_m}{dz}\right|_{z=h}\right) \Big/ \left(2\beta\varphi_m(z=h) - \kappa\right) \qquad \text{(Eq 3-14)}$$

$$c_{2c} = \kappa S_{cc} \left(\frac{3}{2} + \frac{1}{2}\left(1 + 4r \cdot S_{cc}\right)^{1/2} - \frac{2\beta^2 L_c}{\varphi_c(z=h)} \left.\frac{d\varphi_c}{dz}\right|_{z=h}\right) \Big/ \left(2\beta\varphi_c(z=h) - \kappa S_{cc}\right) \qquad \text{(Eq 3-15)}$$

The stability functions $\varphi_{m(c)}$ can be taken from different formulations found in the literature (Arya 2001). In this work, we use a formula for the stability functions that according to Arya (2001, p 218, equation 11.9) can be recommended for most practical applications:

$$\begin{aligned} &\varphi_c = \varphi_m^2 = \left(1 - 15\varsigma\right)^{-1/2}, \quad \varsigma < 0 \,(unstable) \\ &\varphi_c = \varphi_m = 1 + 5\varsigma, \qquad\quad \varsigma \geq 0 \,(stable) \end{aligned} \qquad \text{(Eq 3-16)}$$

3.3 Methods for solution of the model equations

In HF08, the concentration equations were solved analytically. However, in the present work due to different boundary conditions (Equation 3-3 to 3-5) and different source terms (right hand side of Equations 3-1 to 3-2), the analytical solution of the Equations 3-1 to 3-5 is not possible. Therefore, we use numerical methods for solving these equations. Generally, if the simulation domain (in the vertical) can be divided into a large number of boxes (cells), then the finite-difference method can be used. If the number of boxes is restricted to a relatively small number, then the resistance approach can be applied, which requires analytical or numerical integration of the inverse diffusion coefficient between the lower and upper boundaries of each box. Below we describe both approaches, as far as both of them have been used in the present study.

3.3.1 Finite difference approach

Below we show how Equations 3-1 to 3-5 are solved using the finite-difference approach. The computational domain (i.e. range of heights from 0 to z_r) is divided into a number of N cells with the vertical size of each cell being: $h = z_r/N$. Each i-th cell is characterized by concentrations C_i, C^{14}_i. The derivatives in Equations 3-1 to 3-2 are represented with finite differences and the discretized form of the equations is the following:

$$-\frac{K_{c,i+1/2}\left((C_{i+1}-C_i)/h\right)-K_{c,i-1/2}\left((C_i-C_{i-1})/h\right)}{h}=S_{R,i}-S_{P,i} \qquad \text{(Eq 3-17)}$$

$$-\frac{K_{c,i+1/2}\left((C^{14}_{i+1}-C^{14}_i)/h\right)-K_{c,i-1/2}\left((C^{14}_i-C^{14}_{i-1})/h\right)}{h}=-\frac{C^{14}_i}{C_i}S_{P,i} \qquad \text{(Eq 3-18)}$$

where,

$K_{c,i+1/2} = K_c(z_{i+1/2}) = K_c(h(i+1/2))$ – is the diffusion coefficient at the height corresponding to the middle of the interval between the i-th and i+1-th cells. The same definition is applied to $S_{R,i}$, $S_{P,i}$. Equations 3-17 to 3-18 are applied for all nodes ranging from i = 2 to i = N-1, i.e. to all nodes except i = 1 and i = N, representing lower and upper boundaries.

The upper boundary conditions (Equation 3-3) are expressed as:

$$C_N = C_r\,,\ C^{14}_N = 0 \qquad \text{(Eq 3-19)}$$

The lower boundary conditions (Equation 3-4 to 3-5) are expressed as:

$$-K_{c,1/2}\left(C_2-C_1\right)/h = R_0 \qquad \text{(Eq 3-20)}$$

$$-K_{c,1/2}\left(C^{14}_2-C^{14}_1\right)/h = Q_s \qquad \text{(Eq 3-21)}$$

Note that Equation 3-17 is solved independently and prior to the Equation 3-18, since the solution to the latter depends on the solution of Equation 3-17 (there is C_i in the right hand side of Equation 3-18).

Both equations could be expressed in matrix form:

$$\mathbf{A}\bar{C} = \bar{b} \qquad \text{(Eq 3-22)}$$

The elements of vector $\bar{C}$ are the values of concentration (C or C^{14}) in the i-th cell. In the case of CO_2 concentration C, following from Equations 3-17, 3-19 and 3-21 the values of the vector $\bar{b}$ are: $b_i = S_{R,i} - S_{P,i}$ for $1 < i < N$ and $b_N = C_r$, $b_1 = R_0$. The values of matrix $\mathbf{A} = (a_{ij})$ are the following:

$a_{i,j} = 0$ when $j \neq i$, $j \neq i \pm 1$, $a_{ii} = \dfrac{K_{c,i+1/2} + K_{c,i-1/2}}{h^2}$, $a_{ii+1} = \dfrac{-K_{c,i+1/2}}{h^2}$, $a_{ii-1} = \dfrac{-K_{c,i-1/2}}{h^2}$ for $2 < i < N$. For $i = N$: $a_{N,j} = 0$ when $j \neq N$, $a_{NN} = 1$. For $i = 1$: $a_{1,j} = 0$ when $j \neq 1, j \neq 2$, $a_{1,1} = \dfrac{K_{c,1/2}}{h}$, $a_{1,2} = \dfrac{-K_{c,1/2}}{h}$

Analogous formulas, with slight deviations, could be also derived for matrix representation of the equations for C^{14}. Thus, the solution of Equations 3-17 to 3-21 is reduced to the solution of the system of linear Equations 3-22. This can be performed by many methods, such as by Gaussian elimination.

3.3.2 Resistance approach

When cell sizes are relatively large the approximation of turbulent flux with finite differences: $\mathrm{Flux}_{i+1/2} = -\dfrac{K_{c,i+1/2}\left(C_{i+1} - C_i\right)}{h}$ introduces a large error, because $K_{c,i+1/2}$ refers to one specific point (middle of a cell) while K_c could significantly change through the layer between the lower and upper boundaries of a cell. In this case, a reasonable solution is obtained using the resistance approach in which the turbulent flux is represented as: $\mathrm{Flux}_{i+1/2} = -\dfrac{\left(C_{i+1} - C_i\right)}{r_{H,i+1/2}}$, where the resistance of a layer between the centers of the i-th and the i + 1-th cells is defined as:

$$r_{H,i+1/2} = \int_{z_i}^{z_{i+1}} \frac{dz}{K_c} \qquad \text{(Eq 3-23)}$$

If the integral in Equation 3-23 is taken analytically, the resistance approach combined with the increased sizes of cells leads to a significant decrease of computational time. For the relationships Equation 3-8, 3-11 to 3-15, used in HF08, analytical integration is not possible. Therefore, in the present work, the HF08 approach is used only in combination with the finite-difference approach. In the case of the assessment model, substituting the relationships for the turbulent diffusion coefficient above the canopy layer: $K_c = (\kappa/S_c)\, u_*(z-d)$, and inside the canopy layer: $K_c\left(z\right) = K_c\left(h_c\right)\exp\left[\nu_e\left(\dfrac{z}{h_c} - 1\right)\right]$ we obtain the following relationships for the resistances:

$$r_{H,i+1/2} = \int_{z_i}^{z_{i+1}} \frac{dz}{K_c} = \int_{z_i}^{z_{i+1}} \frac{dz}{\left(\kappa / S_c\right) u_*\left(z-d\right)} = \qquad \text{for } z_i > h_c \qquad \text{(Eq 3-24)}$$

$$\frac{z_{i+1} - z_i}{\left(\kappa / Sc\right) u_*}\left[\ln\left(z_{i+1} - d\right) - \ln\left(z_i - d\right)\right] = \ln\left(\frac{z_{i+1} - d}{z_i - d}\right)$$

$$r_{H,i+1/2} = \int_{z_i}^{z_{i+1}} \frac{dz}{K_c} = \int_{z_i}^{z_{i+1}} \frac{dz}{K_c\left(h_c\right)\exp\left[\nu_e\left(\dfrac{z}{h_c} - 1\right)\right]} =$$

$$= \left(\frac{1}{K_c\left(h_c\right)}\right)\int_{z_i}^{z_{i+1}} \exp\left[-\nu_e\left(\frac{z}{h_c} - 1\right)\right] dz = \qquad \text{for } z_{i+1} < h_c \qquad \text{(Eq 3-25)}$$

$$= \left(\frac{h_c}{K_c\left(h_c\right)\nu_e}\right)\left(\exp\left(-\nu_e \frac{z_1 - h_c}{h_c}\right) - \exp\left(-\nu_e \frac{z_2 - h_c}{h_c}\right)\right)$$

When $z_i = 0$ and $z_{i+1} = h_c$, i.e. the resistance represents the whole canopy layer, it becomes: $r_{H,1/2} = (h_c/(K_c(h_c)v_e))(\exp(v_e) - 1$.

As an example, we will approximate Equation 3-7, which represents the fluxes of C^{14}, using the resistance approach. Let N_0 denote a number of the cell which upper boundary coincides with the top of the canopy.

$$\frac{C_i^{14}-C_{i+1}^{14}}{r_{hi+1/2}}=Q_s-\frac{P(h_c)}{C_r}\frac{h}{h_c}\left\{0.5\left(C_1^{14}+C_{i+1}^{14}\right)+\sum_{j=2}^{i}C_j^{14}\right\},\quad i+1<N_0(below\,h_c) \qquad \text{(Eq 3-26)}$$

$$\frac{C_i^{14}-C_{i+1}^{14}}{r_{hi+1/2}}=Q_s-\frac{P(h_c)}{C_r}\frac{h}{h_c}\left\{0.5\left(C_1^{14}+C_{N_0}^{14}\right)+\sum_{j=2}^{N_0-1}C_j^{14}\right\},\quad i+1>N_0(above\,h_c) \qquad \text{(Eq 3-27)}$$

Equations 3-26 to 3-27 are complemented with boundary condition $C_N^{14}=0$ and, as above, they are represented in matrix form: $\mathbf{A}\bar{C}_{14}=\bar{b}$ and solved numerically by the Gaussian elimination method.

Note that in Equations 3-26 to 3-27 we make a simplification by using a constant reference CO_2 concentration C_r in the denominator of the right hand side of the equations, instead of using C_j, which represents the varying CO_2 concentration with height. It will be shown in Chapter 5 that this simplification does not lead to any significant error. This means that in the modeling of the C-14 distribution, the concentration of CO_2 can be assumed to be constant in height.

Using the resistance approach allows a reduction in the number of computational cells by a factor of about 10, while still preserving almost the same accuracy as obtained with the finite difference method. The computational load of the methods used to solve the linear system of equations depends nonlinearly on the number of cells. As a result, the resulting number of operations required to solve the system of equations is reduced by a factor of about 100 with use of the resistance method.

3.4 Summary of model parameters

In practice, the list of input parameters is somewhat flexible and depends upon available data for a particular study. The following basic parameters can be identified, some of which can be further parameterized.

Morphological parameters

a – frontal leaf area per unit volume (function of LAI and h_c)

h_c – canopy height

K_e – extinction coefficient

Meteorological parameters

L – depending on context: Monin-Obukhov length or size of the canopy field

U_h – wind velocity at canopy height

c_d – drag coefficient at the leaf level.

r – leaf level Stanton number

S_{cc} – turbulent Schmidt number inside canopy $\beta = u_*/U_h$

Parameters related to concentration fluxes

P_F – net photosynthesis flux of CO_2

R_F – net respiration flux of CO_2

R_0 – net respiration flux at surface (z = 0)

C^r – reference concentration

z_r – reference height

Q_s – flux ot ^{14}C at soil surface.

4 Validation of the Lagrangian model

In this chapter we present the results of the validation of the Lagrangian model presented in Chapter 3. The validation consisted of comparing vertical profiles of CO_2 predicted with the model with profiles measured in two research stations, one located on a forested area and another on a wheat field.

4.1 Model validation using data from the Norunda Research Station

The Norunda research station (Lundin et al. 1999, Lagergren et.al. 2005) was established in 1994 and is operated by Lund University. The site is covered by a boreal forest of about 25 m height, dominated by Norway spruce and Scots pine. The Leaf Area Index (LAI) typically varies from 3 to 6. The topography is nearly flat. The research station has a 102 m high tower, with eddy flux instrumentation at 35 m. Concentration measurements of CO_2 are taken at 12 levels between 8 and 102 m height. In addition, a wide range of radiation and meteorological parameters are measured; in particular Monin-Obukhov length is provided as well as velocity and temperature profiles.

4.1.1 Selection of model parameter values

The basic parameters required by the HF08 model are listed in Section 3.4. In the following we present the values assigned to these parameters for the model validation exercise. For the conditions of the Norunda site, the value of the frontal area per unit volume a was estimated by least-squares fitting of the theoretical velocity profile inside the canopy to vertical velocity profiles measured at Norunda station over 3 years (2007–2009) with respect to parameter a. This resulted in the value of $a = 0.14$. Note that the value of $a = 0.14$ estimated for Norunda coincides with the value of $a = 0.14$ estimated in HF08 by least-squares fitting to velocity measurements performed in another pine forest (Duke forest), which is characterized by a LAI = 3.8, which is very close to that of Norunda.

The values of r and c_d were taken from HF08 ($r = 0.1$ and $c_d = 0.25$). In HF08, the reference value for β under neutral stratification is provided: $\beta = 0.3$. The average value of this parameter estimated from processing of the measurements collected at Norunda station was the same. Thus, in the present study, this parameter had been set to constant $\beta = 0.3$ for all stability conditions.

Studies of S_{cc} are very limited and some preliminary estimations conducted in HF08 indicate the dependence of S_{cc} on stability conditions (according to HF08 S_{cc} changes from 0.2 for unstable stratification to 0.8 for stable stratification). Existence of such dependence is generally confirmed in the present work, but the particular values of S_{cc} are slightly different from those proposed in HF08 as will be shown below.

Besides setting the turbulence characteristics inside the canopy, the source/sink distribution is to be assigned. In nighttime photosynthesis is absent and only respiration is active. In the present study we have used direct measurements of CO_2 flux at the canopy height. During daytime both respiration and photosynthesis are active and the measurements performed at Norunda represent net CO_2 flux (F_N) through the top of the canopy.

During nighttime the net flux measured above the forest corresponds to the net respiration flux. During daytime the net respiration flux is parameterized using an empirical relationship obtained on the basis of measurements performed at Norunda by Lindroth et.al. (1998) (Figure 5 in the referenced work) as a function of temperature:

$$R_F = 1.64\exp(0.097\mathrm{t}) \qquad \text{(Eq 4-1)}$$

where R_F is in $\mu mol/m^2 s$ (this explains the difference in multiplying coefficient as compared to Lindroth et.al. (1998) where R_F is given in $mg/m^2 s$). It is further assumed that 50 % of the respiration flux originates from the soil surface (according to Lankreijer et al. (2009), the CO_2 respiration flux originates mostly from the surface of the soil) and the rest, 50 %, of the respiration flux is uniformly distributed through the canopy height.

The net photosynthesis flux (P_F) is taken as the difference between net CO_2 flux through the upper boundary of the canopy and the net respiration flux: $P_F = F_N - R_F$. The photosynthesis uptake was assumed to occur between heights of 18 to 25 m. In a study by Jansson et al. (1999), a value of 0.6 was estimated for the extinction coefficient at the Norunda site. Using this value in the equation of radiation decay in the canopy (Equation 15.11 in Arya (2001) corresponding to the Beer's law), it can be estimated that the lower 2 m of canopy absorbs only about 1.5 % of the incoming photosynthetically active radiation. Therefore, the photosynthesis uptake by the ground vegetation has been neglected in this study.

To account for decay of photosynthesis flux with decreasing height 3 layers inside canopy were identified: δ_1 = [18 m, 20 m], δ_2 = [20 m, 22 m], δ_3 = [22 m, 25 m], which produced the following fractions of the net photosynthesis flux: $\alpha_1 = 0.1$, $\alpha_2 = 0.3$, $\alpha_3 = 0.6$. Within each layer the photosynthesis source rate did not change.

4.1.2 Comparison of model simulations with measured data

The simulations were performed in a domain extending vertically up to reference height z_r = 73 m from which measured CO_2 concentrations were taken as reference values and were used to specify the upper boundary condition. That height was chosen because the above-canopy similarity functions had to be validated, but at the same time similarity relationships at higher levels could frequently be violated. The time interval of calculations covered 3 years from 01 Jan 2007 to 31 Dec 2009 with the vertical profiles being measured each 30 minutes. The calculations were performed through the simulation period with a 30 min time step, the meteorological data measured at the corresponding time step were used in simulations and after completion of the simulations the obtained concentrations were averaged.

The simulations were performed separately for daytime conditions (for neutral, slightly unstable and moderately unstable stratifications) and for nighttime conditions (for neutral, slightly stable and moderately stable stratifications). The daytime and nighttime conditions were defined by the value of photosynthetically active radiation (the zero value was considered as nighttime conditions). Nearly calm conditions ($u_* < 0.01$ m/s) as well as the conditions with rain and with very small net fluxes ($|F_N| < 0.1$ μmol/m^{2}s) were not modeled.

The neutral stratification was defined by the threshold condition for Monin-Obukhov Length: $|L| > 500$ m. The slightly stable (unstable stratification) was defined by the range of L: 250 m $< |L| <$ 500 m. The moderately stable (unstable) stratification was defined by the range of L: 70 m $< |L| <$ 250 m. The ranges of L for different stability categories roughly corresponded to the data from Golder (1972). The stronger stability conditions ($|L| <$ 70 m) were not studied, because with such conditions the validity of the stability functions (Equation 3-16) is doubtful.

The results of model application for the case of neutral daytime conditions are shown in Figure 4-1, where vertical profiles of the averaged normalized concentrations $\langle (C(z) - C(z_r))/c_* \rangle$ are shown. First of all, it should be noted that if only the measured net concentration flux is used in the calculations, without partitioning it to photosynthesis and respiration fluxes (the 'no respiration' profile in Figure 4-1), then we could not reproduce the 'counter-gradient' behavior of the concentration profile close to the ground. The observed 'counter-gradient' behavior is the result of non-uniform vertical distribution of photosynthesis and respiration fluxes. The increase of concentrations in the bottom part of the forest canopy, observed in day time conditions when concentration flux above canopy is negative, could be explained by accumulation of CO_2 in the lower part of canopy (originating due to respiration mainly from soil as stated by Lankreijer et al. (2009), combined with the decreased turbulent mixing near the ground.

Figures 4-1 to 4-6 show the results of model simulations compared with measure data. As it generally follows from the results presented in Figures 4-1 to 4-6, the HF08 model gives satisfactory CO_2 profiles both above and inside the canopy layer. Best estimate values of S_{cc} have been obtained by fitting the calculated concentration profiles to the measured profiles. In the case of neutral conditions (Figures 4-1 and 4-2) as well as for slightly or moderately stable conditions (Figures 4-3 and 4-4) and slightly to moderately unstable conditions (see Figures 4-5 and 4-6) the following 'best' values of S_{cc} were obtained: $S_{cc} = 0.2$ for neutral conditions, $S_{cc} = 0.3$ for slightly stable conditions, $S_{cc} = 0.4$ for moderately stable conditions and $S_{cc} = 0.1$ for slightly and moderately unstable conditions.

Hence, it can be concluded that the HF08 parameterization has been successful in reproducing vertical profiles of CO_2 concentrations for daytime and nighttime conditions and for different stability conditions (from neutral to moderately stable and to moderately unstable). Successful results in reproducing the observed CO_2 profiles within the forest canopy in daytime conditions could only be achieved when appropriate values of the respiration flux values were used.

According to measurements, the reduction of the inside canopy concentrations in daytime conditions and under unstable stratification as compared to daytime neutral stratification is −25 % in the bottom of the canopy layer, −15 % in the middle of the canopy layer and nearly 0 % at the top of the canopy layer. Taking into account that the dominating daytime stratification in the region of interest is neutral (the average daytime value of Monin-Obukhov Length is about 800 m), the approximation made in the C14-SVAT model of neglecting stability effects is acceptable for the time scales (season or year) that are relevant for the SR-PSU safety assessment. It also does not lead to underestimation of C-14 concentrations in the canopy layer.

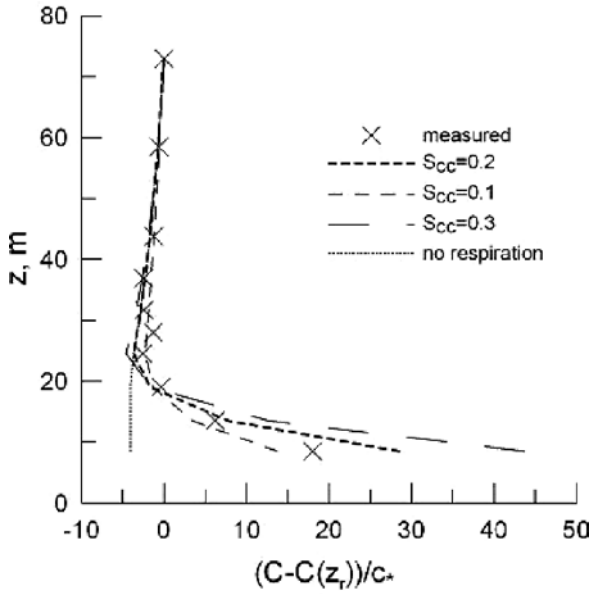

Figure 4-1. *Calculated and measured values of the normalized and averaged vertical profiles of CO_2 concentration for the case of daytime conditions and neutral stratification $|L| > 500$ m.*

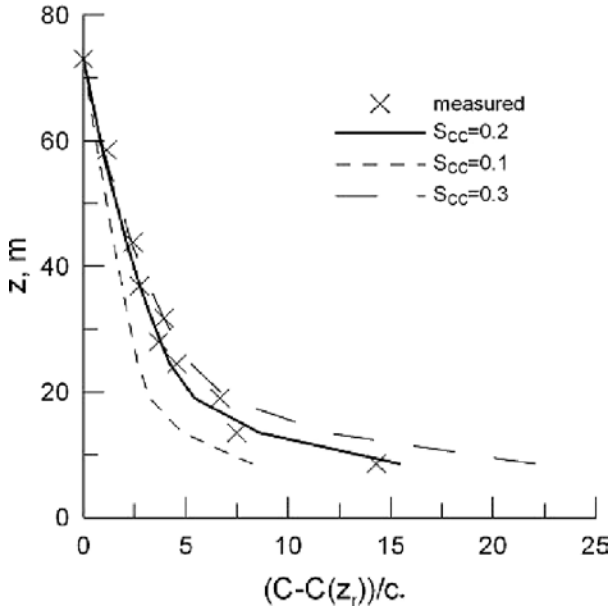

Figure 4-2. *Calculated and measured values of the normalized and averaged vertical profiles of CO_2 concentration for the case of nighttime conditions and neutral stratification $|L| > 500$ m.*

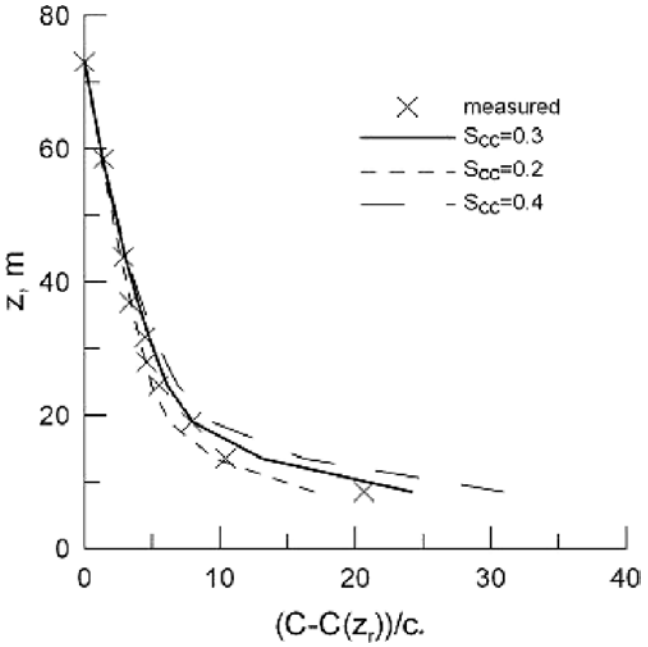

Figure 4-3. *Calculated and measured values of the normalized and averaged vertical profiles of CO_2 concentration for the case of nighttime conditions and slightly stable stratification 250 m $< L \leq$ 500 m*

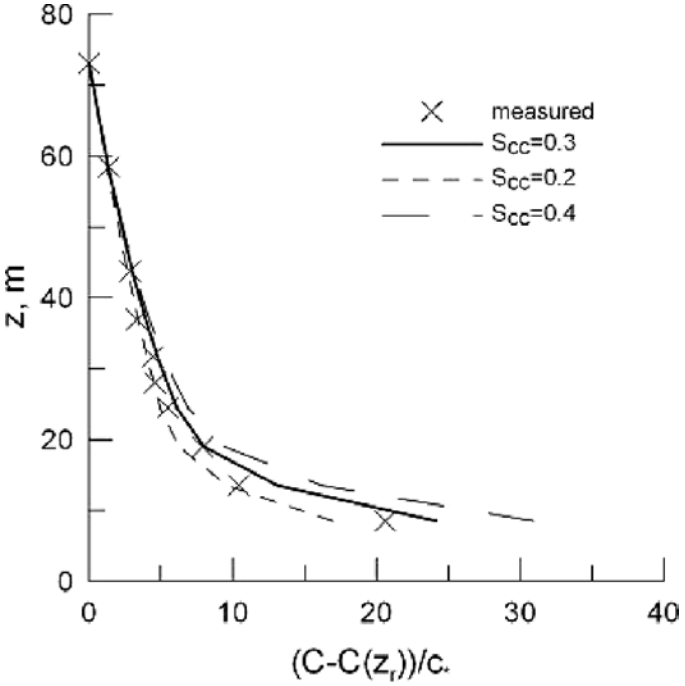

Figure 4-4. *Calculated and measured values of the normalized and averaged vertical profiles of CO_2 concentration for the case of nighttime conditions and moderately stable stratification 70 m $< L \leq$ 250 m*

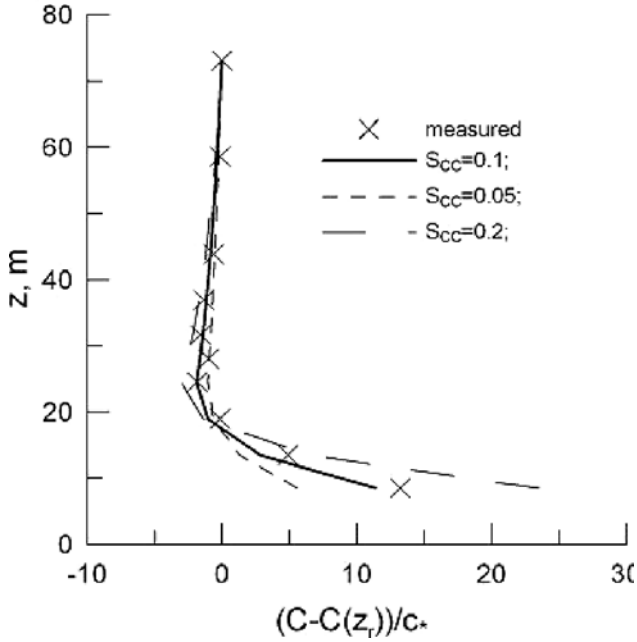

Figure 4-5. *Calculated and measured values of the normalized and averaged vertical profiles of CO_2 concentration for the case of daytime conditions and slightly unstable stratification −500 m ≤ L<−250 m.*

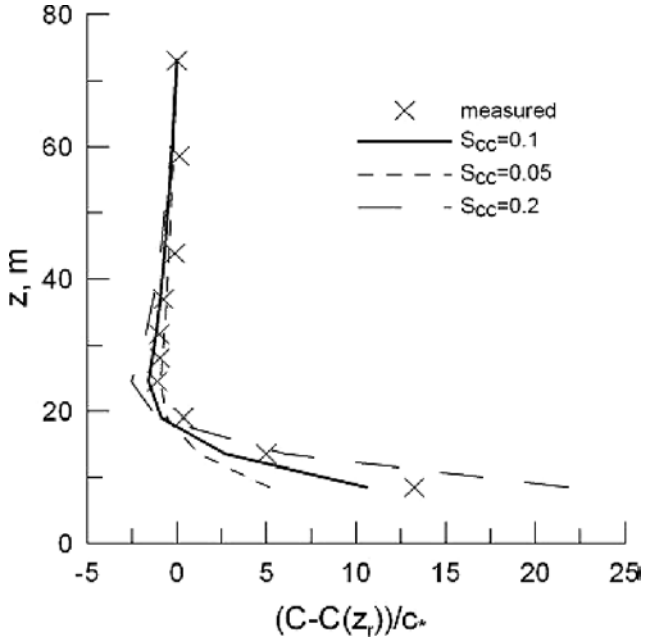

Figure 4-6. *Calculated and measured values of the normalized and averaged vertical profiles of CO_2 concentration for the case of daytime conditions and moderately unstable stratification −250 m ≤ L<−70.*

4.2 Model testing against CO_2 profiles measured above wheat

The exponential profiles of the turbulent diffusion coefficient inside the canopy used in the process level model described in Chapter 3, as well as in the assessment model described in Chapter 2 were derived assuming an infinitely deep canopy and that all momentum is absorbed by the canopy elements and not by the underlying soil. Therefore, even though the validity of the HF08 parameterization for a forest canopy has been demonstrated in the previous section, it is also necessary to demonstrate its validity for other types of canopies.

In contrast to CO_2 profile measurements inside and above forest canopies, such as those collected at Norunda station and at other stations of the FLUXNET network, measurements of CO_2 concentrations inside other types of canopies, such as wheat or barley are practically absent (at least the authors of the present report could not find such publications). Measurements of CO_2 concentrations above, but sufficiently close to the top of canopies, such as wheat or barley are very scarce and rarely published in a form that sufficiently detailed for their usage in modeling work. One of the works which includes a limited set of measurements sufficient for this modeling study is the paper by Shuhua et al. (1998), which presents measurements of CO_2 concentrations and fluxes above wheat collected at the Beijing Agro-Ecosystems Experimental Station (hereafter refereed as Beijing AEES).

4.2.1 The dataset from the Beijing Agro-Ecosystems Experimental Station

The experiment was carried out during summer 1985 at the Agro-Ecosystems Experimental Station (AEES) near Beijing, China. A winter wheat field was used in this experiment. The data obtained during two separate days of the experiment (May 23 and June 23) are available for modeling. Each day represents a different period of the wheat development (the name of the periods is taken from the original paper of Shuhua et al. (1998): 'Earring' (May 23 and 'Ripening' (June 23). The actual experiment covered 10 days, but the paper of Shuhua et al. (1998) does not present sufficient data for modeling other days than those mentioned above. The following data are available from Shuhua et al. (199)] for the days selected for modeling: CO_2 concentrations at heights of 1, 2 and 10 m, as well as momentum and heat fluxes.

4.2.2 Model set up and simulation results

In the previous chapter, it was shown that stratification effects are not of primary importance for the modeling of concentration profiles close to the canopy. Additionally, for almost all measurements presented in Shuhua et al. (1998), the Monin-Obukhov length scale L was greater than 10 m and the computational domain in this study was restricted to the lowest 10 m (because the highest measurement level of concentration was at 10 m). For the above reasons, stratification effects have been neglected in this study.

The data used in the model simulations are presented in Table 4-1. As upper boundary condition, we used the daily averaged data of CO_2 concentration at 10 m C (10 m). For comparisons of calculated results with measurements we used daily averaged concentrations at the height 1 m C (1 m), because hourly concentration measurements were not available for the whole day. Input concentration and momentum fluxes, which are required for modeling the hourly measurements, were available and were used in the modeling.

Table 4-1. Data of the Beijing AEES processed from Shuhua et al. (1998) and used in the present modeling study.

Month	Day	Hour	Concentration flux 10^{-6} kg/(m^2:s)	Momentum flux kg/(m.s)	C (1 m), daily averaged, ppm	C (2 m), daily averaged, ppm	C (10 m), daily averaged,ppm
5	23	9	1.6	0.03	346.3	353.8	374.4
5	23	10	1.8	0.04			
5	23	11	2.1	0.08			
5	23	12	2.2	0.17			
5	23	13	2.1	0.2			
5	23	14	1.85	0.18			
5	23	15	1.5	0.14			
5	23	16	1	0.12			
5	23	17	0.8	0.11			
5	23	18	0.4	0.08			
6	13	8	0.08	0.09	335.5	338.4	348.2
6	13	10	1	0.1			
6	13	12	1.2	0.18			
6	13	14	1.2	0.23			
6	13	16	0.08	0.16			

For the conditions of the wheat canopy the value of the frontal area per unit volume a can be estimated as:

$$a = \frac{2}{\pi}\frac{LAI}{h_c} \qquad \text{(Eq 4-2)}$$

The above formula assumes that plant material is more or less uniformly distributed over height and that wheat could be well approximated by a cylindrical form with diameter D of the stem. Then by definition LAI is half of the total area of the plant's surface per unit ground area: $LAI = \pi D h_c/2$ and the frontal projection of the area is given by Equation 4-2. The LAI for wheat is approximately 2–3.

The values of the leaf-level Stanton number and drag coefficient (r and c_d) are not expected to vary significantly between different plants. But, at the same time, measurement data for these parameters are very scarce. Therefore, the values provided in HF08 were used in the modeling: $r = 0.1$ and $C_d = 0.25$. For the parameter β the value of 0.3 estimated by Brunet et al. (1994) for wheat was used.

Since studies on the value of turbulent Schmidt number inside plant canopies are very limited, the values of S_{cc} were varied in the calculations. Also, since exact information about the LAI of winter wheat was not available in Shuhua et al. (1998), we varied the LAI from 2 to 3. The canopy height was fixed at the value of 1 m.

Table 4-2 presents results of calculations of 1-m CO_2 concentrations for different values of the parameters LAI and S_{cc}. The table also presents the value of the mean relative error:

$$Err = \left\langle \left(C_m(1\ m) - C_o(1m) \right) / \left| C_o(1m) - C_o(z_r) \right| \right\rangle \qquad \text{(Eq 4-3)}$$

In the definition of the mean relative error we divide the difference between the simulated (C_m) and observed (C_o) CO_2 concentrations at the height of 1 m by the difference between the observed concentrations at heights of z_r = 10 m and 1 m. This choice is for two reasons. First, the value of C_o(1 m) ≈ 300 ppm (see Table 4-1) and therefore normalization on just C_o(1 m) would always result in small values of the relative error. Second, if instead of CO_2 we were calculating C-14 then we would had set as the upper boundary condition: $C^{14}(z_r) = 0$. Then the definition (Equation 4-3) would transform to the usual definition of mean relative error:

$$Err = \left\langle \left(C_m^{14}(1\ m) - C_o^{14}(1m) \right) / C_o^{14}(1m) \right\rangle \qquad \text{(Eq 4-4)}$$

Hence, the value of error in CO_2 concentration obtained with Equation 4-3 would be presumably close to the value of error in C-14 concentration obtained with Equation 4-4. As can be seen from the results presented in Table 4-2, the absolute value of mean relative error for the 3 days is less than 15 % if $S_{cc} = 0.3$ and LAI = 2.625. Note that the value of $S_{cc} = 0.3$ is consistent with the values of S_{cc} estimated in the previous section for the case of the Norunda forest. Thus, from the results presented it can be concluded that the HF08 parameterization is applicable for estimation of atmospheric dispersion above such canopies as those of wheat or barley.

Table 4-2. Results of calculations of daily-averaged CO_2 concentrations at the top of wheat for 3 different days and for different values of the LAI and S_{cc}.

S_{cc}	LAI	Err. 23 May	Err. 5 Jun	Err. 13 June	C (1 m). ppm 23 May	C (1 m). ppm 5 Jun	C (1 m). ppm 13 June
0.3	2.25	−0.06629	−0.0868	0.167408	344.4373	338.4655	337.6261
0.3	2.625	−0.12832	−0.15002	0.118968	342.6941	337.5035	337.0109
0.3	3.0	−0.18224	−0.20497	0.076871	341.1792	336.6675	336.4763
0.4	2.25	−0.17506	−0.19766	0.082478	341.3809	336.7789	336.5475
0.4	2.625	−0.23709	−0.26089	0.034037	339.6377	335.8169	335.9323
0.4	3.0	−0.29101	−0.31584	−0.00806	338.1227	334.9809	335.3976
0.5	2.25	−0.25524	−0.27938	0.019866	339.1277	335.5354	335.7523
0.5	2.625	−0.31728	−0.34261	−0.02858	337.3844	334.5734	335.1371
0.5	3.0	−0.37119	−0.39756	−0.07067	335.8695	333.7375	334.6025

5 Evaluation of the C14-SVAT model

In Chapter 4 we presented results of verification of the Lagrangian model using measurements of CO_2 profiles inside and above the canopy of a pine forest and above a wheat canopy. In this chapter, we present results of a study of the sensitivity and similarity of C-14 vertical profiles, generated with the Lagrangian model, with respect to input parameters. This study provides an insight on how simplifying parameterizations and assumptions implicit in the C14-SVAT model affect the predictions made with this model. We also verify the performance of the resistance approach with a decreased grid resolution, which is the approach implemented in the C14-SVAT model.

5.1 Sensitivity of C-14 vertical profiles to model parameters

Simulations of the C-14 vertical profiles were carried out for the same model settings that were used in the validation exercise in Section 4.2, which considered the atmospheric surface layer above a wheat field. The upper boundary condition was set at a reference height z_r = 10 m. Two cases were studied, with and without consideration of lateral advective transport. The finite difference approach was applied to solve the equations of the Lagrangian model using a fine grid resolution of 0.1 m. Below we present non-dimensional concentration profiles of C-14:

$$\tilde{C}(z) = C^{14}(z) u_* / Q_s \qquad \text{(Eq 5-1)}$$

It will be shown that they are almost insensitive to the dimensional parameters of the problem u_* and Q_s.

5.1.1 Case of horizontally homogeneous canopy (no advection)

Simulations for a Reference Case were performed using the values of meteorological parameters from the experiment in Beijing on 5 May. 09 h. described in previous section (see Table 4-1), namely: friction velocity u_* = 0.16 m/s. net CO_2 concentration flux at the top of the canopy $F_N = 1.6 \times 10^6$ kg/m^{2}s , reference CO_2 concentration $C_r = C(10\text{ m}) = 374.4$ ppm. The C-14 flux was taken as Q_s = 1 Bq/m^{2}s. The values given to other parameters for the reference run were: z_r = 10 m, r = 0.1, c_d = 0.25, β = 0.3, a = 1, S_{cc} = 0.3.

Figure 5-1 shows the vertical profiles of the non-dimensional concentration $\tilde{C}(z)$ for for the following cases:

1) Reference Case;
2) In the simulations C-14 is treated as a tracer, i.e. a zero value is used in right hand side of Equation 3-2;
3) The values of the parameters u_* and Q_s are varied;
4) Using a constant in the height profile of CO_2 concentrations, with a value equal to C_r;
5) Variation of the reference height value (z_r = 50 m);
6) Variation of the value of the frontal leaf area per unit volume (a = 2);
7) Variation of the value of the turbulent Schmidt number inside canopy (S_{cc} = 0.5).

Table 5-1 shows the values of non-dimensional concentrations at heights 0.1, 1 and 2 meters obtained for the different cases.

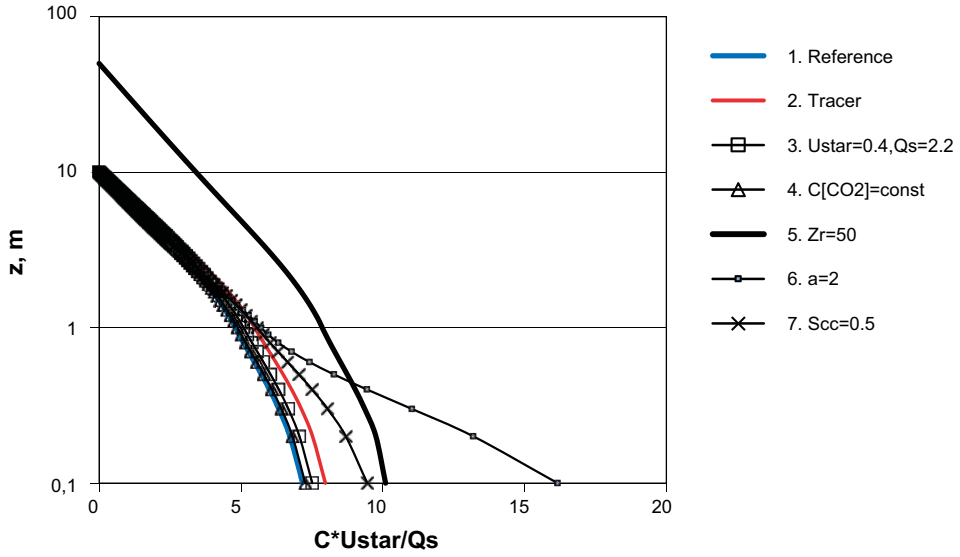

Figure 5-1. *Vertical profiles of the non-dimensional concentration $\tilde{C}(z) = C^{14}(z)\, u_*/Q_s$ for the reference case and for different variations from the reference case listed in text.*

Table 5-1. Values of the non-dimensional concentration at heights 0.1, 1 and 2 meters above ground for different cases listed in text.

No.	Case	$\tilde{C}$ (0.1 m)	$\tilde{C}$ (1 m)	$\tilde{C}$ (2 m)
1	Reference Case	7.17	4.8	3.69
2	Tracer	7.98	5.48	4.22
2a	Tracer, Ust = 0.4 m/s, Qs = 1 Bq/m^{2}s	7.98	5.48	4.22
2b	Tracer, Ust = 0.1 m/s, Qs = 2.2 Bq/m^{2}s	7.98	5.48	4.22
3	Ust = 0.4 m/s; Qs = 2.2 Bq/m^{2}s	7.51	5.09	3.91
3a	Ust = 0.4 m/s, Qs = 1 Bq/m^{2}s	7.6623	5.2156	4.0103
3b	Ust = 0.1 m/s, Qs = 2.2 Bq/m^{2}s	6.6799	4.3842	3.3710
4	C[CO2] = const	7.27	4.88	3.75
5	z_r = 50 m	10.1	7.86	6.84
6	a = 2	16.16	5.7	3.92
7	S_{cc} = 0.5	9.45	5.56	3.92

The following conclusions can be drawn from the obtained results:

- The vertical profile of the non-dimensional concentration is nearly self-similar for release rates of the order of Qs ~1 Bq/m^2.s. For the case in which C-14 is treated as a tracer (Cases 2a and b), self-similarity is exact, as shown in Table 5-1. The reason for deviations from self-similarity of the solution of the full Equation 3-2 lies in the right hand side of this equation, which corresponds to the photosynthesis uptake of C-14. For relatively small concentrations of $^{14}CO_2$, as compared to stable CO_2 concentrations, the self-similarity holds relatively well.
- The assumption made in the C14-SVAT model that C-14 behaves as a tracer introduces an error of no more than 15 % in the calculated C-14 concentration profiles. The concentrations in all three layers for this case are higher than in the Reference Case. So, it can be concluded that this assumption leads to a minor overestimation of the C-14 concentrations by the C14-SVAT model. In the C14-SVAT model, a constant CO_2 concentration in height is assumed in the calculations of C-14 transport and uptake by photosynthesis. Comparisons of the simulation results for this case with the Reference Case showed that this assumption can lead to only a very small error (less than 5 %) in the calculated vertical profiles of C-14.

- The results of calculations are moderately sensitive to the value of turbulent Schmidt number inside the canopy S_{cc}. Variation of this parameter within its confidence interval (i.e. from $S_{cc} = 0.3$ in the reference case to $S_{cc} = 0.5$) leads to changes in the non-dimensional concentrations of up to 30 %.
- The frontal leaf area per unit volume (the parameter a, which is proportional to LAI) has the greatest influence on the estimates of the non-dimensional concentration inside the canopy. Doubling of the value of a (with unchanged net photosynthesis flux) leads to almost doubling of the near-ground value of $\tilde{C}$ due to decreased value of the diffusion coefficient according to Equation 3-10. However, with height the influence of this parameter vanishes: at the height of 1 m doubling of a leads to an increase of $\tilde{C}$ by only 15 %. This parameter is included explicitly in the C14-SVAT model.
- The reference height z_r (i.e. the height at which the C-14 concentration is set to zero, height of L2 in the C14-SVAT model) has a significant influence at all heights and can lead to underestimation of the C-14 concentrations by up to a factor of 2. Hence, it is important that sufficiently high values are given in the C14-SVAT model to the height of the L2 layer. However the sensitivity to the height diminishes when advection is considered on a relevant spatial scale (see below).

5.1.2 Case of canopy field of limited horizontal size (with advection)

As far as the results at Figure 5-1 appeared to be sensitive to the reference height z_r we have also studied the influence of taking into account advection on the simulation results. When advection is not taken into account, the canopy field is assumed to have infinite horizontal length. The effect of the advective transport depends on the horizontal scale of the canopy field. To illustrate this, simulations for two different canopy fields were performed, with length of the horizontal scale of 100 m and 1000 m, respectively.

The results of simulations are presented at Figure 5-2 and in Table 5-2 for the following cases: runs with no advection and with different reference heights of $z_r = 10$ m and $z_r = 50$ m (the same as in previous subsection); runs with advection with varying reference height (as above) and horizontal size of the field (L = 100 m and L = 1000 m). The meteorological conditions in the runs were taken the same as in previous runs, which correspond to a velocity at canopy height $U_h = 0.53$ m/s and a velocity at 10 m height approximately equal to 2 m/s.

As can be seen from the obtained results, advection leads to smoothing of differences between the results obtained with different reference heights. For the size of the canopy field L = 1000 m the difference between runs with different reference heights is already only about 20 % (while without advection the difference was by a factor of about 2). For the size of canopy field L = 100 m the difference becomes even less – only about 1 %. These results show that the effect of the height of the L2 layer in the predictions with the C14-SVAT model is more important when applying the model to large canopy fields.

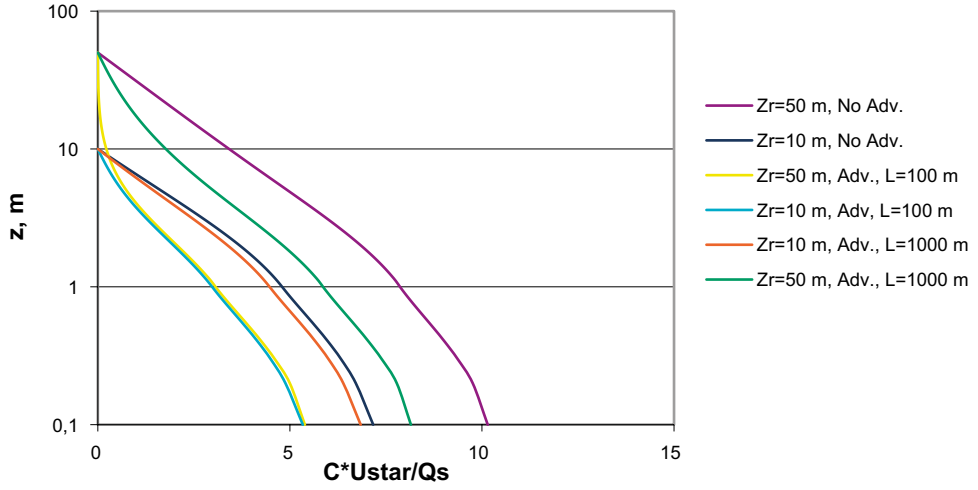

Figure 5-2. *Vertical profiles of the non-dimensional concentration $\tilde{C}(z) = C^{14}(z)\, u_*/Q_s$ for the cases without advection (infinite horizontal length of the canopy) and for the cases with advection over a canopy field of limited horizontal length L.*

Table 5-2. Values of the non-dimensional concentration at heights 0.1, 1 and 2 meters above ground corresponding to the results presented in Figure 5-2.

No.	Note	$\tilde{C}$ (0.1 m)	$\tilde{C}$ (1 m)	$\tilde{C}$ (2 m)
1	Zr = 50 m. No advection	10.1	7.86	6.84
2	Zr = 10 m. No advection (Reference case)	7.17	4.8	3.69
3	Zr = 50 m. Advection. L = 100 m	5.39	3.06	2.06
4	Zr = 10 m. Advection. L = 100 m	5.33	2.98	1.97
5	Zr = 10 m. Advection. L = 1000 m	6.84	4.47	3.38
6	Zr = 50 m. Advection. L = 1000 m	8.15	5.86	4.81

5.2 Verification of the resistance approach

In this section we present a study of the potential impact on the predictions with the C14-SVAT model of two simplifications inherent to this model: the use of simpler relationships for the eddy diffusion coefficients and only three layers are used to model the vertical turbulent transport with the resistance approach.

Parameterization of the eddy diffusion coefficients

The C14-SVAT model uses somewhat simpler relationships for the eddy diffusion coefficients (see Section 2.1.6) derived from the similarity theory under neutral stratification (e.g. Garratt 1992). These relationships do not take into account the above-canopy influence of the RSL. The advantage of using this simplified parameterization, as compared with the parameterization in HF08, follows from the possibility of their analytical integration which allows using the 'resistance' approach in the numerical procedure of solving the diffusion problem. Below we evaluate the effect of this simplified parameterization on the model predictions.

First, for the Reference Case described above, we compare the results obtained with the C14-SVAT model, described in Chapter 2, against the results obtained with the Lagrangian model, described in Chapter 3 and verified in Chapter 4. The value of the extinction coefficient for wheat was set at: $v_e \approx 2.6$ (Campbell and Normann 1998). Two methods for calculating the eddy diffusion coefficient at the top of the canopy were used in the C14-SVAT model: In the first method (used in the current version of the C14-SVAT model described in Chapter 2), Equation 2-12 was used, which ensures continuity at the top of the canopy; whereas in the second method (used in the Lagrangian model), Equation 3-10 was used, which accounts for increase of the turbulent mixing at the top of the canopy.

Figure 5-3 and Table 5-3 show the vertical profiles of the non-dimensional concentration calculated using the Lagrangian model with the HF08 parameterization and using the C14-SVAT model with the two methods described above for calculation of the eddy diffusion coefficient at the canopy top.

As follows from the results presented in Figure 5-3 and Table 5-3, the current C14-SVAT model overestimates the concentration near the ground surface by a factor of about 3, and underestimates the concentration at 2 m and 1 m by a factor of about 1.7 and 1.6, respectively. The results with the C14-SVAT model when using method 2 are much closer to the results with the Lagrangian model and reproduce the concentration at 1 m with an accuracy of a few percent. Hence, it should be considered whether to change the parameterization of the eddy diffusion coefficient in the C14-SVAT model from method 1 to method 2, although this may require that numerical integration methods are applied to obtain the eddy diffusion coefficients in the 3 atmospheric layers considered in the model.

Table 5-3. Values of the non-dimensional concentration at heights 0.1, 1 and 2 meters above ground obtained with the Lagrangian model for the Reference Case and with the C14-SVAT model using methods 1 and 2 for parameterization of the eddy diffusion coefficients at the canopy height.

Model	$\tilde{C}$ (0.1 m)	$\tilde{C}$ (1 m)	$\tilde{C}$ (2 m)
Lagrangian model	7.17	4.8	3.69
C14-SVAT model. Method 1	20.45	3.02	2.11
C14-SVAT model. Method 2	9.44	4.75	2.72

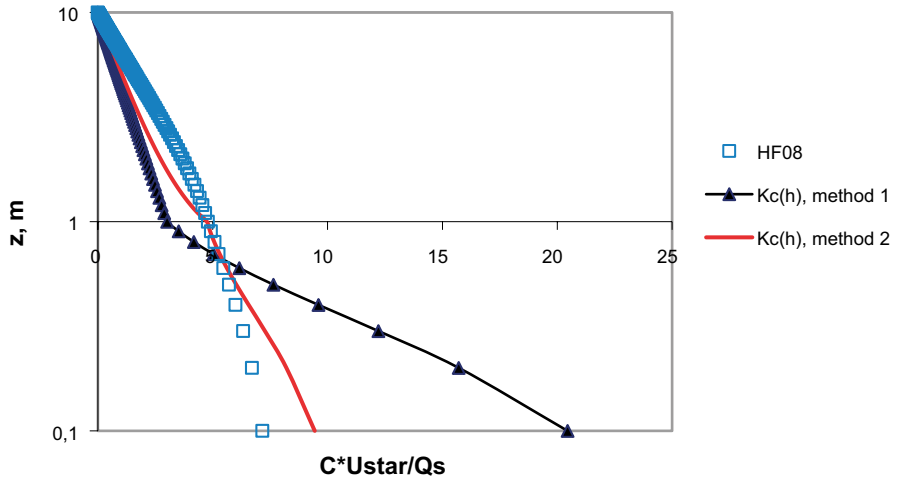

Figure 5-3. *Vertical profiles of the non-dimensional concentration $\tilde{C}(z) = C^{14}(z)\, u_*/Q_s$ for the Reference Case. Results shown were obtained with the Lagrangian model (HF08) and with the C14-SVAT model using method 1 and method 2 (see text) for parameterization of the eddy diffusion coefficient at the canopy height.*

Evaluation of the resistance approach

The results obtained with the Lagrangian model and presented above were obtained using the finite difference approach for solving the model equations with a fine grid resolution of 0.1 m; i.e. with 100 computational cells. We also evaluated the effects on the results of decreasing the grid resolution by applying the resistance approach described in Section 3.3.2. Table 5-4 presents the different mesh configurations that were used in the study.

Table 5-4. Heights of computational cells used in the calculations with the Lagrangian model when applying the approach based on resistances using four different mesh configurations.

Cell No.	Conf. 1 Bottom height, m	Conf. 2 Bottom height, m	Conf. 3 Bottom height, m	Conf. 4 Bottom height, m
1	0	0	0	0
2	1	0.2	0.5	1
3	2	0.4	1	2
4	10	0.6	2	3
5	–	0.8	4	4
6	–	1.0	6	5
7	–	2	8	6
8	–	3	10	7
9	–	5	–	8
10	–	10	–	9
11	–	–	-	10

The results from calculations for the Reference Case obtained with the Lagrangian model for the four mesh configurations (Table 5-4) and using the resistance approach are presented in Figure 5-4, where the results obtained from the finite difference method with a fine grid resolution of 0.1 m (100 computational cells) are also presented. It can be seen that using Configuration 1, with only 3 computational cells (as it is the case in the current C14-SVAT model), leads to an overestimation of the concentrations by about a factor of 3. Increasing the resolution in the lowest 1 m layer (Configuration 2) reduces the overestimation of the concentrations, but the results still differ substantially from the results using the finite difference method. This is because the increase in the size of the cells (up to 5 m) at the upper levels in Configuration 2 leads to an overall increase in the error of the simulations. The same is valid for Configuration 3. The results obtained for Configuration 4, with 1 m resolution (10 cells) equally distributed from 0 to 10 m, are practically identical to the results

obtained with the finite difference method. Thus, using the resistance approach allows a decrease in the grid resolution by a factor of 10 as compared with using the finite difference approach. These results also indicate that the predictions with the C14-SVAT model could be substantially improved (and reduce the overestimation) if Configuration 4 is adopted, which could be achieved by discretizing the atmospheric layer L2 into 8 layers with a thickness of 1 m each.

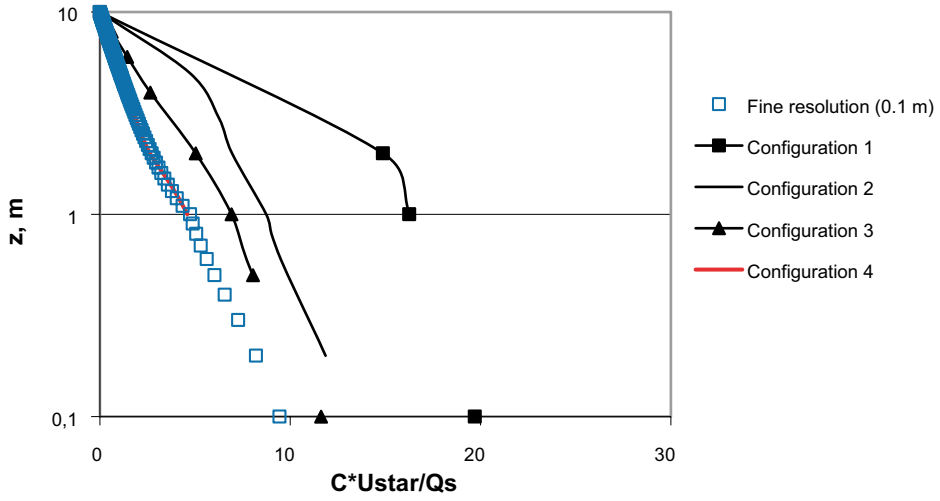

Figure 5-4. *Vertical profiles of the non-dimensional concentration $\tilde{C}(z) = C^{14}(z)\, u_*/Q_s$ for the Reference Case calculated with the Lagrangian model using the finite difference approach with a fine resolution (0.1 m) and using the resistance approach with coarser resolutions (configurations 1-4 according to Table 5-4).*

6 Conclusions

In this report we present an assessment model (the C14-SVAT model) of the C-14 transport in the surface atmosphere above vegetated land that receives releases of this radionuclide from the soil (see Section 2.1). The model is applicable for all vegetation types that are incorporated in the SR-PSU biosphere model: crops like cereals, tubers, vegetables as well as for fodder and mire vegetation. It can be used for making predictions for relevant endpoints in a safety assessment of radioactive waste disposal facilities, such as C-14 concentrations and specific activities in the air that humans breathe and in plants, which are used in the calculation of inhalation and food ingestion doses, respectively.

The C14-SVAT model represents an improvement of a similar model (Avila and Pröhl 2008) that has been used in preceding safety assessments (SAR-08 and SR Site). The main improvement has entailed integrating explicit modelling of the turbulence driven transport of C-14 in the atmosphere within and above the canopy. The C14-SVAT model is a relatively simple analytical model that is fit for purpose in the context of safety assessments. This came at the price of introducing various simplifications in the model. We have evaluated the implications of these on the accuracy of the model predictions with the help of a Lagrangian model, which we developed specially for this purpose.

The Lagrangian model is based on the LNF theory as described in Harman and Finnigan (2008). It can simulate with a high resolution the turbulent transport of CO_2 and C-14 in the surface atmosphere and their interactions with the canopy. We validated this model with two datasets of CO_2 atmosphere vertical profiles, one obtained over a boreal forest in the Norunda research station (Lundin et al. 1999, Lagergren et.al. 2005) and another obtained over a wheat field in the Beijing Agro-Ecosystems Experimental Station (Shuhua et al. 1998). We then performed simulations with the Lagrangian model for a number of cases to evaluate the potential impact of the assumptions made in the C14-SVAT model on the predictions with this model.

From the evaluations made we conclude that, provided that the diffusivity coefficient at canopy top is assigned properly, the simplifying assumptions implicit in the C14-SVAT model do not lead to underestimations of the C-14 concentrations within the canopy layer, and some of them lead to moderate overestimations. From the evaluation we also identify possible ways of improving the model predictions while still keeping the model simple. One possible improvement could be to represent the above-canopy atmosphere with a larger number of layers (around nine). Another could be to adopt the same parameterization of the eddy diffusion coefficient as in the Lagrangian model, although this might require numerical integration to obtain the values for the different layers.

In this report, we also present an assessment model (the C14-WAT model) of the C-14 transport in the atmosphere above surface waters from where this radionuclide can be released by degassing. The model can be used for calculation of C-14 concentrations in air above the water surface, which can be then used in estimation of inhalation doses during swimming and boating.

References

SKB's (Svensk Kärnbränslehantering AB) publications can be found at www.skb.com/publications.

Allen R G, Pereira L S, Raes D, Smith M, 1998. Crop evapotranspiration – Guidelines for computing crop water requirements. Rome: Food and Agriculture Organization of the United Nations (FAO irrigation and drainage paper 56). Available at: http://www.fao.org/docrep/X0490E/x0490e00.htm#Contents

Amiro B D, Ewing L L, 1992. Physiological conditions and uptake of inorganic carbon-14 by plant roots. Environmental and Experimental Botany 32, 203–211.

Arya S P, 2001. Introduction to micrometeorology. 2nd ed. San Diego: Academic Press.

Avila R, Pröhl G, 2008. Models used in the SFR 1 SAR-08 and KBS-3H safety assessments for calculation of C-14 doses. SKB R-08-16, Svensk Kärnbränslehantering AB.

Baldocchi D D, Verma S B, Rosenberg N J, 1983. Microclimate in the soybean canopy. Agricultural Meteorology 28, 321–337.

Belcher S E, Harman I N, Finnigan J J, 2012. The wind in the willows: flows in forest canopies in complex terrain. Annual Review of Fluid Mechanics 44, 479–504.

BIOPROTA, 2011. C-14 long-term dose assessment: data review. scenario development. and model comparison. DRAFT FINAL REPORT. Main contributors: Limer L M C, Smith K, Albrecht A, Marang L, Norris S, Smith G M, Thorne M C and Xu S.

Brunet Y, Finnigan J J, Raupach M R, 1994. A wind tunnel study of air flow in waving wheat: single-point velocity statistics. Boundary-Layer Meteorology 70, 95–132.

Campbell G S, Normann G M, 1998. An introduction to environmental biophysics. 2nd ed. New York: Springer.

Finnigan J, 2000. Turbulence in plant canopies. Annual Review of Fluid Mechanics 32, 519–571.

Garratt J R, 1980. Surface influence upon vertical profiles in the atmospheric near-surface layer. Quarterly Journal of the Royal Meteorological Society 106, 803–819.

Garratt J R, 1992. The atmospheric boundary layer. Cambridge: Cambridge University Press.

Golder D, 1972. Relations among stability parameters in the surface layer. Boundary-Layer Meteorology 3, 47–58.

Grolander S, 2013. Biosphere parameters used in radionuclide transport modelling and dose calculations in SR-PSU. SKB R-13-18, Svensk Kärnbränslehantering AB.

Harman I N, Finnigan J J, 2007. A simple unified theory for flow in the canopy and roughness sublayer. Boundary-Layer Meteorology 123, 339–363.

Harman I N, Finnigan J J, 2008. Scalar concentration profiles in the canopy and roughness sublayer. Boundary-Layer Meteorology 129, 323–351.

Hoch A R, 2014. Uptake of gaseous carbon-14 in the biosphere: development of an assessment model. AMEC/004041/007, Issue 2, AMEC.

Jansson P E, Cienciala E, Grelle A, Kellner E, Lindahl A, Lundblad M, 1999. Simulated evapotranspiration from the Norunda forest stand during the growing season of a dry year. Agricultural and Forest Meteorology 98–99, 621–628.

Kustas W P, 1990. Estimates of evapotranspiration with a one- and two-layer model of heat transfer over partial canopy cover. Journal of Applied Meteorology 29, 704–715.

Kuzyakov Y, Domanski G, 2000. Carbon input by plants into the soil. Journal of Plant Nutrition and Soil Science 163, 421–431.

Lagergren F, Eklundh L, Grelle A, Lundblad M, Mölder M, Lankreijer H, Lindroth A, 2005. Net primary production and light use efficiency in a mixed coniferous forest in Sweden. Plant, Cell & Environment 28, 412–423.

Lankreijer H J M, Lindroth A, Strömgren M, Kulmala L, Pumpanen J, 2009. Forest floor CO_2 flux measurements with a dark-light chamber. Biogeosciences Discussions 6, 9301–9329.

Lide D R, 2008. CRC Handbook of Chemistry and Physics, 89th ed. CRC Press, Boca Raton, FL.

Lindroth A, Grelle A, Moren A-S, 1998. Long-term measurements of boreal forest carbon balance reveal large temperature sensitivity. Global Change Biology 4, 443–450.

Lundin L-C, Halldin S, Lindroth A, Cienciala E, Grelle A, Hjelm P, Kellner E, Lundberg A, Mölder M, Morén A-S, Nord T, Seibert J, Stähli M, 1999. Continuous long-term measurements of soil–plant–atmosphere variables at a forest site. Agricultural and Forest Meteorol 98–99, 53–73.

Mölder M, Grelle A, Lindroth A, Halldin S, 1999. Flux-profile relationships over a boreal forest-roughness sublayer corrections. Agricultural and Forest Meteorology 98–99, 645–658.

Nobel P S, 2009. Physicochemical and environmental plant physiology. 4th ed. Amsterdam: Elsevier Academic Press.

Raupach M R, 1989. A practical Lagrangian method for relating scalar concentrations to source distributions in vegetation canopies. Quarterly Journal of the Royal Meteorological Society 115, 609–632.

Sharkey T D, 1988. Estimating the rate of photorespiration in leaves. Physiologia Plantarum 73, 147–152.

Sheppard M I, Sheppard S C, Amiro B D, 1991. Mobility and plant uptake of inorganic ^{14}C and ^{14}C-labelled PCB in soils of high and low retention. Health Physics 61, 481–492.

Shuhua L, Leclerc M Y, Xu Mei, Ma Yimin, 1998. Concentration and flux of CO_2, turbulence fluxes and radiation balance in the near surface layer of the wheat field. Acta Meteorologica Sinica 12, 221–234.

Shuttleworth W J, Gurney R J, 1990. The theoretical relationship between foliage temperature and canopy resistance in sparse crops. Quarterly Journal of the Royal Meteorological Society 116, 497–519.

Shuttleworth W J, Wallace J S, 1985. Evaporation from sparse crops – an energy combination theory. Quarterly Journal of the Royal Meteorological Society 111, 839–855.

Tagesson T, 2012. Turbulent transport in the atmospheric surface layer. SKB TR-12-05, Svensk Kärnbränslehantering AB.

Vourinen A H, Vapaavuori E M, Lapinjoki S, 1989. Time-course of uptake of dissolved inorganic carbon through willow roots in light and darkness. Physiologia Plantarum 77, 33–38.

Wilson J D, 1989. Turbulent transport within the plant canopy. In Black T A (ed). Estimation of areal evapotranspiration: proceedings of an international workshop held during the XIXth General Assembly of the International Union of Geodesy and Geophysics at Vancouver. British Columbia. Canada, 9–22 August 1987. Wallingford: International Association of Hydrological Sciences.

Wilson J D, Sawford B L, 1996. Review of Lagrangian stochastic models for trajectories in the turbulent atmosphere. Boundary-Layer Meteorology 78, 191–210.

Appendix 1

Nomenclature used in the equations of the Lagrangian model

This appendix presents the nomenclature that is used in the equations of the process level model described in Chapter 3.

A – matrix in the representation of the system of linear equations

a – frontal leaf area per unit volume

$\bar{b}$ – right-hand side vector in the matrix representation of a system of linear equations

C, $C(z)$, C_j CO_2 concentration in air at height z or at level j

C^{14}, $C^{14}(z)$, C_j^{14} concentration in air of radioactive carbon (^{14}C) at height z or at level j

C' – turbulent fluctuation of concentration

C_m, C_o – simulated ('m') and observed ('o') concentrations

C^r – reference concentration

c_* – concentration flux scale.

c_d – drag coefficient at the leaf level.

$\bar{c}$ – vector of concentrations in the matrix representation of a system of linear equations

D – stem diameter

d – displacement height

Err – mean relative error

F_D – drag force inside the canopy

F_N – net CO_2 flux through the upper canopy boundary $f = \frac{1}{2}(1+4rScc)^{1/2} - \frac{1}{2}$

g_c – leaf level boundary-layer conductance for scalar transfer

h – vertical mesh size

i, j – indices

K_e – extinction coefficient

$K_{m(c)}$ – turbulent exchange coefficient for momentum (index 'm') or scalar (index 'c')

L – depending on context: Monin-Obukhov length or size of the canopy field

LAI – accumulated leaf area index

$L_c = (a \cdot c_d)^{-1}$ – length scale of absorption of momentum by the canopy

$l_{m(c)}$ – mixing lengths for momentum and for concentration

N – number of cells in the vertical direction

N_0 – cell number with a height that coincides with the height of the canopy

P_F – net photosynthesis flux

$P(z)$ – photosynthesis flux at height z

Q_s – flux of ^{14}C at the soil surface

$q_{m(T,c)}$ – turbulent momentum. heat and scalar fluxes at canopy height. $q_m = \langle u'w' \rangle|_{z=h}$.

$q_T = \langle T'w' \rangle|_{z=h}$. $q_c = \langle C'w' \rangle|_{z=h}$ where primes denote fluctuation components and triangle brackets denote time averaging.

r_H – resistance of the layer

R_F – net respiration flux

$R(z)$, R_0 – respiration flux at height z or at surface (z = 0)

r – leaf level Stanton number

S_c – turbulent Schmidt number: $S_c = K_m/K_c$

S_{cc} – turbulent Schmidt number inside canopy

S_P, $S_P(z)$, S_p^k – photosynthesis source rate at height z or at k-th layer

S_R, $S_R(z)$, S_p^k – respiration source rate at height z or at k-th layer

S_χ – absorption (release) rate by canopy elements at a given height z

T – temperature

T' – turbulent fluctuation of temperature

t – temperature in Celsius

U, $U(z)$ – wind velocity

U_h – wind velocity at canopy height

u' – turbulent fluctuation of the wind velocity

u_* – friction velocity

w – leaf half width

w' – turbulent fluctuation of vertical velocity

z_i – height (of i-th node) above ground

z_r – reference height

z_* – height of the roughness sub-layer

α_k – fractions of net photosynthesis flux produced by k-th layer $\beta = u_*/U_h$

β_N – value of β for neutral conditions

β_1 – parameter of the vertical profile $\sigma_w(z)$

δ_k – k-th layer on which canopy layer is sub-divided

$\varphi_{m(c)}$ – stability correction function for $K_{m(c)}$

$\hat{\varphi}_{m(c)}$ – correction function for $K_{m(c)}$ taking into account the roughness sub-layer

$\Phi_{m(c)} = \varphi_{m(c)}\,\hat{\varphi}_{m(c)}$

$\kappa = 0.4$ – von Karman constant

v_e – extinction coefficient (rate of decay of velocity and diffusivity inside canopy)

σ_w – root mean squared value of the vertical velocity fluctuations

$\langle\ \rangle$ – depending on the context: operator of arithmetic averaging or time averaging (when defining turbulent fluxes)